

1 **TITLE:**

2 Diet during early life defines testicular lipid content and sperm quality in
3 adulthood

4 **RUNNING HEAD:** Diet in childhood defines testes' lipid content in adulthood

5 **KEYWORDS:** High-fat diet; early-life obesity, diet intervention; lipidomics; male
6 fertility

7

8 **AUTHORS:**

9 Luís Crisóstomo ^{1,2,3}, Romeu A. Videira ^{1,4}, Ivana Jarak ^{1,4}, Kristina Starčević ⁵,
10 Tomislav Mašek ⁶, Luís P. Rato ⁴, João F. Raposo ^{7,8}, Rachel L. Batterham ⁹,
11 Pedro F. Oliveira ^{1,10}, Marco G. Alves ¹ ✉

12 ¹ Department of Microscopy, Laboratory of Cell Biology, and Unit for Multidisciplinary Research in
13 Biomedicine (UMIB), Institute of Biomedical Sciences Abel Salazar (ICBAS), University of Porto, Portugal;

14 ² Department of Genetics, Faculty of Medicine of the University of Porto (FMUP), Portugal; ³ i3S – Instituto
15 de Investigação e Inovação em Saúde, University of Porto, Portugal; ⁴ Faculty of Health Sciences,

16 University of Beira Interior, Covilhã, Portugal; ⁵ Department of Chemistry and Biochemistry, University of
17 Zagreb, Faculty of Veterinary Medicine, Zagreb, Croatia; ⁶ Department of Animal Nutrition and Dietetics,

18 University of Zagreb, Faculty of Veterinary Medicine, Zagreb, Croatia; ⁷ NOVA Medical School – New
19 University Lisbon, Lisbon, Portugal; ⁸ APDP – Diabetes Portugal, Lisbon, Portugal; ⁹ Centre for Obesity

20 Research, Rayne Institute; Centre for Weight Management and Metabolic Surgery & National Institute of
21 Health Research, University College London, London, UK; ¹⁰ QOPNA & LAQV, Department of Chemistry,

22 University of Aveiro, Aveiro, Portugal

23

24 ✉ Corresponding author:

25 **Marco G. Alves, PhD**

26 Email: alvesmarc@gmail.com

27 Phone: (+351) 967 245 248

28 Address: ICBAS - University of Porto, Department of Microscopy, Rua de Jorge Viterbo Ferreira

29 228, 4050-313 Porto, Portugal.

30

31 Supplemental Material available at

32 URL: <https://figshare.com/s/785af8effa28e8bc2935>

33 DOI: <https://doi.org/10.6084/m9.figshare.12302171>

34

35

36 **ABSTRACT**

37 Childhood obesity is a serious concern associated with ill health later in life.
38 Emerging data suggest that obesity has long-term adverse effects upon male
39 sexual and reproductive health but few studies addressed this issue. We
40 hypothesized that exposure to high-fat diet during early life alters testicular lipid
41 content and metabolism leading to permanent damage to sperm parameters.
42 After weaning (day 21 after birth), 36 male mice were randomly divided into 3
43 groups and fed with different diet regimen for 200 days: CTRL–standard chow;
44 HFD–high-fat diet (Carbohydrate: 35.7%, Protein: 20.5%, Fat: 36.0%); HFDt–
45 high-fat diet for 60 days then replaced by standard chow. Biometric and
46 metabolic data were monitored. Animals were then sacrificed, and tissues
47 collected. Epididymal sperm parameters and endocrine parameters were
48 evaluated. Testicular metabolites were extracted and characterized by ¹H-NMR
49 and GC-MS. Testicular mitochondrial and antioxidant activity were evaluated.
50 Our results show that mice fed with high-fat diet, even if only until early
51 adulthood, had lower sperm viability and motility, and higher incidence of head
52 and tail defects. Although diet reversion with weight loss during adulthood
53 prevents the progression of metabolic syndrome, testicular content in fatty acids
54 is irreversibly affected. Excessive fat intake promoted an over-accumulation of
55 pro-inflammatory n-6 polyunsaturated fatty acids in testis, which are strongly
56 correlated with negative effects upon sperm quality. Therefore, the adoption of
57 high-fat diets during early life correlates to irreversible changes in testicular lipid
58 content and metabolism, which are related to permanent damage to sperm
59 quality later in life.

60

61 **New & Noteworthy**

62 The adoption of high-fat diets from early-age promotes a pro-inflammatory
63 environment in testis, due to the accumulation of n-6 polyunsaturated fatty
64 acids. Diet reversion to standard chow in early adulthood does not revert
65 testicular lipid content completely. This testicular lipid remodeling is correlated
66 to poorer sperm parameters later in life, notably sperm motility, viability and
67 morphological defects. Hence, high-fat diets cause irreversible damage to male
68 reproductive function.

69

70 **INTRODUCTION**

71 The fast and global increase of overweight/obesity in recent decades led the
72 World Health Organization to declare it the “Epidemics of the XXI Century” (72).
73 Excessive fat deposition has been associated with the onset of non-
74 communicable diseases, particularly type 2 diabetes (T2DM) (22). Consumption
75 of energy-dense, high-fat diet (HFD), and low physical activity are two major
76 drivers of the obesity epidemic (22). In developed countries, consumption of
77 energy-dense foods occurs at an ever-younger age (41). Childhood obesity
78 rates continue to soar worldwide, with obesity-associated comorbidities
79 occurring at a younger age (33, 71). Concurrently, concerns on the impact of
80 excessive adiposity and T2DM on sperm quality and fertility outcomes have
81 been raised (14, 42, 51). Although there are not many studies demonstrating
82 the impact of fat-rich diets in sperm quality, men attending fertility centers are
83 often advised to lose weight and adopt a balanced diet. Unlike the other lifestyle
84 interventions such as physical activity (62), the effectiveness of dietary
85 intervention in recovering normal sperm quality or its positive effects on
86 testicular metabolism has never been demonstrated (64).

87 Normal male reproductive function requires a well-orchestrated balance of
88 endocrine and metabolic factors to secure proper energy flow towards meiosis
89 and cellular remodeling of differentiating germ cells (55). In this regard,
90 testicular lipid dynamics are crucial, not only as energy substrates, but also as
91 structural elements of the future sperm cells. Moreover, mitochondrial function
92 and antioxidant defenses are crucial for providing energy for spermatogenesis
93 and sperm motility, while avoiding oxidative damage which can critically
94 compromise cell functions. Previously we have shown that HFD during early life

95 causes irreversible changes in testicular metabolism, even after reversion, and
96 those changes are correlated to defects in sperm motility, viability and
97 morphology (12). The relevance of fatty acids in testicular physiology has been
98 reported, specially the repercussions for spermatogenesis (20, 28, 37, 57). We
99 hypothesize that the adoption of HFDs affects testicular lipid dynamics resulting
100 in poorer sperm quality. We further address whether an HFD early in life can
101 irreversibly affect sperm quality later in life, due to testicular lipid
102 dysmetabolism, even after diet intervention in early adulthood. We have
103 performed our study in a rodent model. Biometry, glucose homeostasis,
104 endocrine function, testicular antioxidant system, testicular bioenergetics and
105 sperm parameters were assessed. We have further performed a multivariate
106 analysis supported by targeted metabolomics and lipidomics, based on semi-
107 quantitative GC-MS and ¹H-NMR, to determine changes in testicular lipid
108 metabolism.

109

110 **MATERIALS & METHODS**

111 *Animal Model*

112 *Mus musculus* C57BL6/J male mice (n=36) were randomly divided into three
113 groups after weaning (21-23 days): control (CTRL) (n=12), HFD (n=12) and
114 transient HFD (HFD_t) (n=12). All mice were generated from normoponderal
115 males and females and were subjected to the same random *in utero* stimuli,
116 although generated from different litters. Briefly, CTRL group mice were fed with
117 a standard chow (#F4031, BioServ, USA – Carbohydrate: 61.6%, Protein:
118 20.5%, Fat: 7.2% - 16.3% Kcals). HFD group mice received a HFD (#F3282,

119 BioServ USA – Carbohydrate: 35.7%, Protein: 20.5%, Fat: 36.0% - 59.0%
120 Kcals) for 200 days after weaning. HFD_t group mice were fed with a HFD
121 (#F3282, BioServ, New Jersey, USA) for 60 days and then switched to standard
122 chow (#F4031, BioServ, New Jersey, USA). At 120 days post-weaning, mice
123 were randomly assigned to a normoponderal female, in mating pairs, 6 hours
124 per day, for seven consecutive days, for breeding. During this period, female
125 breeders were kept in the same standard diet. Mating pairs had no access to
126 water or food during mating (6h). Reproductive success rate, litter size, and
127 litter male to female ratio were assessed. Animals were killed by cervical
128 dislocation 200 days after weaning, and tissues collected for further analysis.
129 Total body weight, water and food intake were monitored weekly until sacrifice.
130 The animal model is compliant with the ARRIVE guidelines and was licensed by
131 the Portuguese Veterinarian and Food Department (0421/000/000/2016).

132

133 *Endocrine and metabolic function*

134 Fasting glycemia was measured before sacrifice (200 days post-weaning), after
135 overnight fast (8h), using a glucometer (One Touch Ultra Lifescan-Johnson,
136 Milpitas, CA, USA) by collecting a drop of blood from the tail vein. Blood was
137 then collected by cardiac puncture and centrifuged at 1500 g, 4 °C, for 10
138 minutes to collect the serum. Serum insulin was quantified using a Rat/Mouse
139 Insulin ELISA assay (EZRMI-13K, Millipore). Glucose homeostasis was
140 evaluated according to the HOMA2 scores (30), using the HOMA2 calculator
141 (University of Oxford, United Kingdom). Disposition index (DI) was calculated as
142 suggested by Caumo et al. (9). Similarly, FSH, LH, 17β-estradiol and

143 testosterone were quantified in the purified serum using ELISA kits
144 (respectively, ENZ-KIT108-0001, ENZ-KIT107-0001, ADI-900-174 and ADI-900-
145 176, Enzo Life Sciences, USA).

146

147 *Evaluation of epididymal sperm parameters*

148 Epididymides were isolated and placed in pre-warmed (37°C) Hank's Balanced
149 Salt Solution (HBSS) pH 7.4, minced with a scalpel blade and the suspension
150 was incubated for 5 min (37°C). Sperm parameters were evaluated as
151 previously described (12, 53). Sperm motility was calculated as the average
152 proportion of motile sperm in 10 random microscope fields, observing a drop of
153 sperm suspension on a warmed slide (37 °C) using an optical microscope
154 (×100 magnification). Epididymal sperm concentration was determined using a
155 Neubauer counting chamber and an optical microscope (×400 magnification), in
156 a diluted the sperm suspension (1:50 in HBSS). Sperm viability and morphology
157 were assessed in differently stained epididymal sperm smears, counting 333
158 spermatozoa in random fields using an optical microscope (×400 magnification).
159 Sperm viability smears were stained with eosin-nigrosin (29), as membrane-
160 compromised spermatozoa stain pink. Sperm morphology smears were stained
161 with Diff-Quick (Baxter Dale Diagnostics AG, Dubinger, Switzerland). Sperm
162 morphology categories were mutually exclusive, *i.e.*, spermatozoa displaying
163 more than one defect were assigned according to the most serious defect
164 category (decapitated > pinhead > flattened head > bent neck > coiled tail) (29).

165

166 *NMR spectroscopy*

167 A combined extraction of polar and nonpolar metabolites from testicular tissue
168 was performed as previously described (2, 12). Testes were washed with saline
169 and decapsulated prior to metabolite extraction to minimize contamination by
170 blood metabolites. The aqueous phase containing polar water-soluble
171 metabolites was lyophilized and analyzed by ¹H-NMR spectroscopy as
172 described (25). Lipid metabolites were identified by comparing recorded spectra
173 with reference spectra and the Human Metabolome Database (HMDB) (69) and
174 according to Metabolomics Standards Initiative (MSI) guidelines for metabolite
175 identification (65). Identification levels are indicated in Table S1 (Supplementary
176 data). ¹H spectra were processed using previously described methods (25).
177 Obtained peak areas were normalized by the total spectral area and analyzed
178 by univariate analysis. Areas were obtained using AMIX software (Bruker
179 BioSpin GmbH, Rheinstetten, Germany) and expressed as arbitrary units
180 defined by the software.

181

182 *GC-MS analysis*

183 Fatty acid methyl esters of total lipids were obtained by base-catalyzed
184 transmethylation (2 M KOH in methanol) in the presence of nonadecanoic fatty
185 acid (C19:0), used as the internal standard. The obtained hexane fatty acid
186 methyl esters solution was analyzed by gas chromatography using a Shimadzu
187 GC-MS QP2010 UltraGas Chromatograph Mass Spectrometer (Shimadzu,
188 Kyoto, Japan), equipped with a capillary column BPX70 (0.25 mm internal
189 diameter, 0.25 μm film thickness, 30 m long, SGE, Austin, TX, USA). The

190 injector temperature was 250 °C, and 1 µl of each sample was injected with a
191 split ratio of 1:80. Helium was used as the carrier gas, and the linear velocity
192 was 35 cm/s. The initial column temperature was 155 °C, followed by a heating
193 rate of 1 °C/min up to 170 °C, 4 °C/min up to 220 °C and 40 °C/min until
194 reaching 250 °C, maintained for 5 min. Linear velocity was 35 cm/s, interface
195 temperature: 250 °C, ion source temperature: 225 °C, mass range: 45-500 and
196 event time: 0.3 s. All the experimental measurements were repeated three
197 times and the average values reported. Fatty acids were identified by retention
198 time and fragmentation profile and quantified by the internal standard
199 procedure. Results were expressed as a percentage of total fatty acids.

200

201 *Lipid peroxidation, activity of antioxidant enzymes and activity of mitochondrial*
202 *enzyme complexes*

203 A single testis from each animal was homogenized in 2 mL of ice-cold
204 extraction buffer [160 mM sucrose, 10 mM Tris–HCl, pH 7.4] supplemented with
205 a protease inhibitors cocktail (#B14001, Bimake, Munich, Germany) (1:10, p/v)]
206 using a glass-Teflon Potter Elvehjem (Kimble, Millville, NJ, USA). The resulting
207 homogenate was split into two fractions: one was used for adenine nucleotides
208 (ATP, ADP, and AMP) extraction and quantification by high-performance liquid
209 chromatography (HPLC), as described (40); the other was fractionated by
210 differential centrifugation to obtain a mitochondria-free cytosolic fraction and a
211 mitochondria-enriched fraction, as described (38, 40). The final protein content
212 of each fraction was determined by the BCA method (61). The mitochondria-
213 enriched fraction was used to assess the activity of the mitochondrial enzymes

214 (complexes I, II and IV, V and citrate synthase), while the mitochondria-free
215 cytosolic fraction was used to evaluate the activity of the enzymes of the
216 antioxidant defense system [catalase (CAT), copper-zinc superoxide dismutase
217 (SOD), glutathione peroxidase (GPx), glutathione-disulfide reductase (GSR)]
218 and to assess the levels of lipid peroxidation.

219 Catalase (CAT) activity was polarographically determined following oxygen
220 production resulting from H₂O₂ decomposition using a Clark-type oxygen
221 electrode (Hansatech, Norfolk, UK) (13). Superoxide dismutase (SOD),
222 glutathione peroxidase (GPx) and glutathione-disulfide reductase (GSR)
223 activities were evaluated in 96-well plates, at 37 °C, as described (46). The
224 reaction was conducted in 930 µL of 100 mM potassium phosphate buffer (100
225 mM KH₂PO₄, 5 mM EDTA, pH 7.4) with 50 µl of testicular cytosol extract, and
226 initiated by adding 20 µl of H₂O₂ (2 mM). CAT activity was expressed in nmol
227 O₂/min/mg protein.

228 SOD activity was evaluated by mixing 50 µl testicular cytosolic fraction with 170
229 µl potassium phosphate buffer, supplemented with 2 mM nitro blue tetrazolium
230 (NBT) and 0.05 U Xanthine Oxidase (#X1875-10UN, Sigma-Aldrich/Merck
231 KGaA, Darmstadt, Germany). After addition of 10 µl hypoxanthine (2 mM),
232 absorbance at 560 nm was measured every 20 seconds for 5 minutes. Results
233 were expressed as U/min/mg protein, where U is the enzyme activity that
234 inhibited the reduction of NBT to blue formazan by 50%.

235 GR activity was evaluated by the rate of NADPH oxidation associated with the
236 reduction of GSSG. Assays were carried out in 170 µl potassium phosphate
237 buffer, supplemented with 10 mM NADPH and 10 mM GSSG. After adding 300
238 µL of testicular cytosolic fraction, NADPH oxidation was recorded by the

239 fluorescence decrease at 450 nm (Excitation: 360 nm) every 20 seconds for
240 5 minutes. NADPH oxidation not associated with GSSG reduction was
241 assessed in assays carried out in the absence of GSSG. GR activity was
242 determined by difference between the rate of NADPH oxidation in the presence
243 and absence of GSSG and expressed in nmol/min/mg of protein.

244 GPx activity was evaluated by the rate of NADPH oxidation associated with
245 H₂O₂ reduction. Assays were performed in 170 µl potassium phosphate buffer,
246 supplemented with 10 mM GSH and 1-3U Glutathione Reductase (#G3664-
247 500UN, Sigma-Aldrich/Merck KGaA, Darmstadt, Germany), and 50 µl of
248 testicular cytosol fraction. Reaction was initiated by the addition of 10 µl H₂O₂
249 (0.6 mM), and fluorescence at 450 nm (Excitation: 360 nm) was measured
250 every 20 seconds for 5 minutes. GPx activity was determined by the rate of
251 NADPH consumption in nmoles/min/mg of protein.

252 Testicular lipid peroxidation levels were evaluated by the production of
253 thiobarbituric acid reactive species (TBARS assay). Shortly, 50 µl testicular
254 cytosolic fraction were mixed with 600 µl of Reaction Solution [thiobarbituric
255 acid 0.38% (m/V), trichloroacetic acid 37% and 2,6-ditertbutyl-4-methylphenol
256 0.02% (m/V) (38)] and incubated at 95 °C for 30 minutes. Malondialdehyde
257 (MDA) formation was measured by colorimetric methods ($\epsilon = 156 \text{ mM}^{-1} \cdot \text{cm}^{-1}$),
258 and results were expressed in nmol MDA/mg protein.

259 Activities of the mitochondrial complexes I, II and IV, and citrate synthase (CS)
260 were assessed, at 37 °C, in 96-well plate by adapting previously described
261 protocols (40). CS was determined spectrophotometrically, by monitoring the
262 reduction of DTNB. The reaction mixture consisted of 200 mM Tris-HCl buffer
263 (pH 8.0), 0.02% Triton X-100, 10M DTNB, 1 mM oxaloacetate, and 20 µl of

264 testicular mitochondrial fraction. The reaction was initiated by adding 0.37 mM
265 acetyl-CoA, and the absorbance at 412 nm was recorded every 30 seconds for
266 10 minutes. CS activity was calculated by DTNB ($\epsilon = 13.6 \text{ mM}^{-1} \cdot \text{cm}^{-1}$) reduction
267 rate, determined in the linear range of the plot, and expressed as nmol/min/mg
268 protein.

269 Complex I activity was assessed following NADH oxidation. The reaction was
270 performed in a potassium phosphate buffer (25 mM KH_2PO_4 , 10 mM MgCl_2 ; pH
271 7.4) supplemented with 1 mM KCN, 162.5 μM decylubiquinone, 3.0 μM
272 rotenone (or equal volume of buffer) and 20 μl of testicular mitochondrial
273 fraction. The reaction was triggered by the addition of NADH (50 μM), and
274 fluorescence at 450 nm (excitation: 366 nm) was measured every 20 seconds
275 for 15 minutes. Complex I activity was determined by the difference between
276 NADH oxidation rate in rotenone-inhibited wells and non-inhibited wells. This
277 value was expressed in nmol NADH/min/mg.

278 Complex II activity was assessed monitoring 2,6-dichlorophenolindo-phenol
279 (DCPIP) reduction at 600 nm ($\epsilon = 20.7 \text{ mM}^{-1} \cdot \text{cm}^{-1}$) in a potassium phosphate
280 buffer, supplemented with 2 mM KCN, 6.5 μM rotenone, 6.5 μM antimycin A,
281 0.05 mM DCIP, 0.1 mM decylubiquinone and 20 μl of testicular mitochondrial
282 fraction. Negative control wells were further supplemented with 0.5 mM
283 oxaloacetate (complex II inhibitor). The reaction was initiated by adding 20 mM
284 succinate and absorbance measure every 30 seconds for 20 minutes. Complex
285 II activity was expressed as the DCPIP reduction rate (corrected for
286 spontaneous reduction) in nmol DCPIP/min/mg protein.

287 Complex IV activity was evaluated by the cytochrome c (CytC) oxidation rate.
288 CytC (50 mM) was fully reduced by the addition of small volumes of saturated

289 sodium dithionite solution. CytC oxidation reaction was performed in extraction
290 buffer, supplemented with 3 μM rotenone, 0.1 μM antimycin A (inhibitor of
291 complex III), 2 mM KCN (specific inhibitor of complex IV) or equal volume of
292 buffer, and 20 μl of testicular mitochondrial fraction. The reaction was initiated
293 by adding 15 μM reduced CytC, and the absorbance at 550 nm was recorded
294 every 15 seconds for 5 minutes. Complex IV activity was calculated by CytC (ϵ
295 = 29.5 $\text{mM}^{-1}\cdot\text{cm}^{-1}$) oxidation rate, corrected by the spontaneous oxidation rate
296 obtained in the KCN-inhibited wells, and expressed as nmol CytC/min/mg
297 protein.

298 Maximal activity of the mitochondrial complex V was measured using a
299 MitoCheck Complex V Activity Assay kit (Cayman Chemical, Ann Arbor, MI,
300 USA). All colorimetric and fluorometric readings described in this section were
301 obtained using a Biotek Synergy H1 plate reader (Winooski, VT, USA).

302

303 *Determination of testicular adenosine nucleotides levels by HPLC*

304 Testicular adenosine nucleotides levels were assessed in a Waters 600 HPLC
305 system (Waters, Milford, MA, USA) equipped with 2487 dual- λ Absorbance
306 Detector. ATP, ADP, and AMP were separated on a reverse-phase
307 chromatography column (Lichrospher[®] RP-18 HPLC Column, 5 μm particle
308 size, L x I.D. 25 cm x 4.6 mm), using a gradient mobile phase that consisted of
309 Phase A (100 mM KH_2PO_4 buffer with 1.2% methanol v/v, pH = 7.0) and Phase
310 B (100 mM KH_2PO_4 buffer with 10% methanol v/v, pH =7.0) The elution
311 program was the following: 100% of A from zero to 20 min followed by a linear
312 gradient up to 100% of B until 25 min, and from 25 to 28 min down to 0% B
313 (initial conditions). The flow was 1 ml/min, and the column temperature was

314 maintained at 25 °C during the run. Chromatograms were recorded at 254 nm,
315 and analyzed using the Waters Millennium32 (Waters, Milford, MA, USA).
316 Peaks were identified by their retention times, comparing them with samples of
317 standard compounds. ATP, ADP, and AMP levels were quantified using
318 standard curves obtained with a serial of known concentrations of each of the
319 adenine nucleotides run on the same day and conditions of the samples. The
320 results were expressed as mol/g wet tissue.

321 *Statistical and exploratory factor analysis*

322 Different statistical methods were applied depending on the objective and the
323 nature of the analyzed data. Kolmogorov-Smirnoff test was used to test data
324 normality. Whenever normality was ensured, one-way ANOVA with Tukey's
325 post-hoc test was set as the default test. Whenever this assumption was
326 violated, extreme values of more than 3 standard deviations from the mean
327 were omitted. Otherwise, the non-parametric Kruskal-Wallis test was performed,
328 using the Mann-Whitney test as a post-hoc test. The overall distribution of
329 sperm defects between groups was further tested using the χ^2 test. The non-
330 parametric Spearman correlation was used to correlate fertility and sperm
331 parameters. The parametric Pearson correlation (r coefficients) was used to
332 correlate the different sets of variables in the study (sperm parameters,
333 endocrine and metabolic function, mitochondrial function, bioenergetics and
334 antioxidant system), after variables were successfully tested for normality using
335 the Kolmogorov-Smirnoff test, and as part of exploratory factor analysis. The
336 correlation strength was classified according to ranks (67). Variables with
337 significant ($p < 0.05$) linear correlation with sperm parameters were then

338 considered for Multivariate Analysis based on Principal Components Analysis
339 (PCA). Although PCA is an unsupervised multivariate method, it was used as a
340 sparse and supervised method considering the variable selection criteria based
341 on linear (Pearson) correlation. Forced factor extraction was performed to
342 extract 2 Principal Components (PCs), based on the interpretability criterion,
343 and using Varimax with Keiser's Normalization as Rotation Method. Regression
344 factors were used to plot sample distribution in the two-dimensional Euclidean
345 space. All methods were performed using IBM SPSS Statistics v25 (Armonk,
346 NY, USA). Independently of the statistical method used, significance was
347 considered whenever $p < 0.05$.

348

349 **RESULTS**

350 *Hormonal balance is not affected by high-fat diets, and glucose homeostasis is*
351 *recovered after dietary correction*

352 In our previous study (12) we found that dietary switch from a fat-rich diet to a
353 standard chow was able to normalize biometric parameters (Figure SF1, panels
354 A and B) and glucose homeostasis (Figure 1). Hereby, we further characterized
355 the model by studying the endocrine function, including insulin and reproductive
356 hormones such as FSH, LH, 17β -estradiol, and testosterone (Table 1). As
357 observed before, the severe impairment in all the parameters related to
358 metabolic homeostasis (HOMA2), significantly improved after diet reversal
359 (Figure 1). HFD mice had a β -cell function approximately 3 and 2-fold higher
360 than those of CTRL and HFD_t (Figure 1a). Influence on glucose sensitivity (%S)
361 (Figure 1b) and insulin resistance (IR) (Figure 1c) was even more pronounced -

362 10 and 5-fold increase was observed in HFD animals when compared to CTRL
363 and HFD_t, respectively. Plasma insulin levels were found to be increased in
364 HFD mice and notably, diet correction restored plasma insulin levels (Table 1).

365

366 *Dietary correction in adulthood after HFD in early life does not restore the*
367 *decreased sperm quality*

368 We collected epididymal sperm immediately after sacrifice. Sperm motility and
369 concentration were promptly assessed according to standard protocols. Sperm
370 viability and morphology were evaluated after specific staining techniques and
371 using optical microscopy. We have found no differences in sperm counts
372 between groups (Figure 2). However, mice fed HFD, even if transiently,
373 displayed reduced sperm motility (CTRL: 81.6 ± 4.6 %; HFD: 69.1 ± 7.4 %;
374 HFD_t: 65.9 ± 14.5 %) and sperm viability (CTRL: 48.2 ± 8.1 %; HFD: 38.1 ± 7.2
375 %; HFD_t: 34.4 ± 6.6 %). Regarding sperm morphology (Table 2), we used three
376 different classification systems: descriptive (6 defects), categorical (3
377 categories) and binomial (normal/abnormal). Based on the χ^2 test, we found that
378 sperm morphology distribution is different between groups. Notably, recurring to
379 ANOVA and Tukey's HSD, we have found differences in the prevalence of
380 pinhead, flattened head, bent neck and overall head defects, especially relative
381 to HFD_t. Despite the observed changes in sperm parameters, diet did not
382 influence reproductive outcomes (Table S2). No significant correlations were
383 found between sperm and fertility parameters (data not shown).

384

385 *Testicular mitochondrial function and bioenergetics are not affected by high-fat*
386 *diets*

387 Mitochondria were isolated from a whole testis to evaluate relevant parameters
388 related to its activity and physiology. Particularly, relative protein expression of
389 mitochondrial OXPHOS complexes was assessed by western blot, and the
390 activities of complexes I, II, IV and citrate synthase were evaluated by
391 colorimetric/fluorometric assays (Table S3). Testicular bioenergetics were
392 evaluated based upon testicular content of adenine nucleotides (ATP, ADP and
393 AMP), quantified by HPLC (Table S4). These nucleotides were extracted from
394 the same testis used to isolate the mitochondria-rich fraction. There were no
395 differences between any of the experimental groups.

396

397 *A high-fat diet promotes a decrease in the activity of antioxidant defenses in*
398 *testis*

399 Lipid peroxidation and activity of enzymes of the antioxidant defense system
400 were evaluated in mitochondria-free cytosolic fraction obtained from a whole-
401 testis homogenate. The dietary regime did not influence testicular levels of lipid
402 peroxidation products (Figure 3a). Additionally, activities of the cytosolic GPx
403 and SOD were similar in the testes of the mice from the different groups (Figure
404 3b and 3c). Conversely, mitochondria-free cytosolic fraction obtained from the
405 testes of HFD group mice exhibited a decrease in CAT (CTRL: 747.66 ± 141.46
406 $\text{nmol O}_2 \cdot \text{min}^{-1} \cdot \text{mg protein}^{-1}$; HFD: $552.41 \pm 91.51 \text{ O}_2 \cdot \text{min}^{-1} \cdot \text{mg protein}^{-1}$;
407 HFD_t: $670.02 \pm 107.21 \text{ O}_2 \cdot \text{min}^{-1} \cdot \text{mg protein}^{-1}$) and GSR activities (CTRL:
408 $133.14 \pm 11.31 \text{ nmol NADPH} \cdot \text{min}^{-1} \cdot \text{mg protein}^{-1}$; HFD: $114.00 \pm 11.53 \text{ nmol}$

409 NADPH . min⁻¹ . mg protein⁻¹; HFD_t: 120.44 ± 9.14 nmol NADPH . min⁻¹ . mg
410 protein⁻¹).

411

412 *Testicular lipid metabolism is irreversibly affected by a HFD during early life*

413 Metabolites were obtained from a whole-testis using a protocol based on
414 chloroform-methanol-water extraction, resulting in a polar and apolar fractions.
415 In the polar fraction, analyzed by ¹H-NMR, various phospholipid-related
416 metabolites and lipid precursors were detected (Table 3). HFD had a marked
417 influence on the composition of polar lipids as observed in the levels of
418 phospholipid head groups like myo-inositol, choline or glycerol, or choline
419 related glycerophosphocholine (GPC). Reversal from HFD to normal diet
420 tended to normalize metabolite levels.

421 The apolar fraction of the testicular extract was characterized by GC-MS after
422 transmethylation. The identified fatty acids (FAs) were quantified and their
423 relative abundance is displayed in Table S5. Dietary intervention promoted a
424 meta-state between CTRL and HFD conditions for most of the identified FAs
425 (e.g: palmitic acid and stearic acid). The only exception was vaccenic acid
426 (C18:1n-7), which is twice more abundant in testes of HFD_t mice than in CTRL.
427 After grouping FAs by degree of unsaturation and the position of the double
428 bonds (Table S5 and Figure 4), we observed that the most abundant FA family
429 in the testis of CTRL and HFD_t groups are the saturated fatty acids (SFAs)
430 (55.79% and 41.83%, respectively), while polyunsaturated fatty acids (PUFAs)
431 are the most abundant in the testis of mice from the HFD group (44.21%). HFD
432 and HFD_t mice had also increased testicular relative abundance of

433 monosaturated fatty acids (MUFAs) (26% and 21%, respectively), with
434 increased accumulation of oleic acid (C18:1n-9). Moreover, Table S5 also
435 shows indirect measures for the anti-inflammatory/pro-inflammatory potential
436 via lipid mediators (C22:6n-3/C20:4n-6 ratio), the combined activity of Δ 5- and
437 Δ 6-desaturases (D5D and D6D) (C20:4n-6/C18:2n-6 ratio), and the activity of
438 Δ 4-desaturases (D4D) (C22:5n-6/C20:4n-6 ratio).

439

440 *Male reproductive dysfunction caused by HFD is correlated to lipid*
441 *dysmetabolism in testes*

442 Our main aim was to evaluate whether a dietary intervention in early adulthood
443 can prevent damage to male reproductive health. However, as in previous
444 studies (12, 25), groups were not considered when testing for correlations.
445 Assuming that all mice are equivalent before being fed by a specific diet
446 regimen, our test hypothesis is that some pairs of variables vary proportionally
447 in response of HFD. Those pairs reflect the most relevant (discriminant)
448 variables, therefore the variables that must be included in the multivariate
449 model. In a correlation matrix (Figure 5A) we tested variables of mitochondrial
450 function, bioenergetics, endocrine function and antioxidant defenses against
451 sperm parameters. We found a significant negative correlation between
452 Complex I activity and the prevalence of pin head sperm defect ($r = -0.577$; $p =$
453 0.024). Regarding bioenergetics, the increase in testicular content in ATP ($r =$
454 0.517 ; $p = 0.034$) and ATP/ADP ratio ($r = 0.592$; $p = 0.012$) was correlated with
455 elevated sperm counts. AMP ($r = -0.638$; $p = 0.011$) and AMP/ATP ratio ($r = -$
456 0.703 ; $p = 0.003$) were inversely correlated to sperm head defects, particularly

457 decapitated sperm ($r = -0.627$; $p = 0.012$ and $r = -0.689$; $p = 0.005$). Conversely,
458 testicular energy charge was positively correlated to both parameters ($r = 0.733$;
459 $p = 0.002$ and $r = 0.633$; $p = 0.011$). Concerning endocrine function, most
460 correlations were found in glucose homeostasis. Elevated serum levels of
461 insulin ($r = -0.425$; $p = 0.043$), HOMA2-%B ($r = -0.523$; $p = 0.010$) and HOMA2-
462 IR ($r = -0.438$; $p = 0.037$) were correlated with lower sperm viability. HOMA2-
463 %S behaved contrarily to the former ($r = 0.424$; $p = 0.044$). FSH showed a
464 protective effect against sperm head defects ($r = -0.464$; $p = 0.039$), namely pin
465 ($r = -0.505$; $p = 0.023$) or flattened head ($r = -0.673$; $p = 0.001$) defects.
466 Concerning antioxidant defenses, only SOD activity presented a significant
467 inverse correlation to sperm concentration ($r = -0.527$; $p = 0.030$). Significantly
468 correlated variables were selected for PCA, to evaluate their predictive power
469 (*i.e.*, if samples were clustered according to their diet using these variables as
470 predictors). These correlations promote a significant clustering of samples
471 according to their experimental group, and there is no overlap between groups,
472 considering 2 PCs (Figure 5B).

473 In the second correlation matrix (Figure 6A), sperm parameters were correlated
474 against testicular lipid metabolite levels. Testicular content in SFAs and PUFAs
475 had a mirror effect over the prevalence of bent neck and coiled tail sperm
476 defects: while SFAs were negatively correlated with bent sperm neck defects (r
477 $= -0.668$; $p = 0.035$) and positively correlated with coiled sperm tail defects (r
478 $= 0.649$; $p = 0.042$). MUFAs had the opposite relation to bent sperm neck (r
479 $= 0.744$; $p = 0.014$) and to coiled sperm tail ($r = -0.663$; $p = 0.037$). Globally, lipid
480 precursors correlated positively with sperm viability. Testicular glycerol (r
481 $= 0.612$; $p = 0.020$) and myo-inositol ($r = 0.592$; $p = 0.026$), however, displayed a

482 positive correlation with the prevalence of bent neck sperm. Choline is positively
483 correlated to normal morphology of sperm ($r = 0.609$; $p = 0.021$), whilst
484 negatively correlated to tail defects ($r = 0.614$; $p = 0.019$). The 2-dimensional
485 projection of the PCs extracted by PCA (Figure 6B) reveal a clear separation of
486 the samples according to their group.

487

488 **DISCUSSION**

489 Overweight and obesity have reached pandemic proportions worldwide.
490 Simultaneously, the prevalence of childhood obesity is increasing, leading to the
491 onset of obesity-associated comorbidities, such as T2DM, at younger ages.
492 Reproductive function depends on metabolic homeostasis. Several reports link
493 the prevalence of metabolic disease with lower sperm quality (14, 19, 51). In
494 this study, we used a rodent model to investigate whether a dietary intervention
495 to replace an HFD with a balanced diet in early adulthood, is effective in
496 reversing or preventing the negative effects of childhood obesity in fat
497 accumulation, metabolic homeostasis, and sperm quality. Particularly, we
498 evaluated if diet intervention is effective in normalizing testicular metabolic and
499 lipid balance, and sperm quality later in life. We further integrated all data of
500 metabolomics and lipidomics to elucidate the importance of lipids in
501 mechanisms involved in the onset and/or recovery of the fertility phenotypes
502 induced by HFD in early life.

503 We have previously demonstrated that this model induces phenotypic traits
504 related to obesity and metabolic syndrome, based on biometric and
505 physiological tests for glucose intolerance (ipGTT) and insulin resistance (ipITT)

506 (12). We have shown that HFD promoted fat deposition in white adipose tissue
507 pads and liver, which were positively correlated with poorer performance in
508 ipGTT and ipITT. In this report we calculated HOMA2 indexes based on fasting
509 glycemia and fasting insulin levels (30). Although HOMA2 application to animal
510 models is often criticized (68) as it has been developed based on a large human
511 database, it has shown an acceptable goodness of fit for mouse and other
512 mammals (4, 5), and has a high correspondence to ipITT, ipGTT and their
513 respective AUCs (1). As its precursor, HOMA, it is based upon serum fasting
514 glycemia and insulinemia, therefore providing a better physiological
515 characterization of glucose homeostasis. The methodology for quantifying
516 hormonal serum concentrations at the sacrifice was ELISA, for all selected
517 hormones. Insulin was the only hormone measured found to be altered when
518 comparing hormonal levels in the serum of mice from the different groups.
519 HOMA2 showed that dietary intervention is not capable to completely reverse
520 the effects of a HFD during early life in β -cell function and insulin sensitivity,
521 despite total recovery of insulin resistance index. Despite these results not
522 being novel (12), it is relevant to state the high correspondence degree with our
523 previous results, obtained using different methods for glucose homeostasis
524 assessment.

525 Although testosterone aromatization into estradiol has been widely reported in
526 patients with obesity, our results support recent research showing that this
527 effect may be negligible (6, 52). Although another study suggests marked
528 changes in sex hormone levels in HFD rodents (8), circulating levels of fertility-
529 related hormones were not influenced by dietary regimes in this particular study
530 (Table 1). Yet, endocrine function is strongly correlated with sperm quality,

531 especially glucose homeostasis and FSH secretion (3, 11, 55) (Figure 5A). In
532 this context, Sertoli Cells (SCs) may be the mediator between both factors and
533 sperm quality. SCs nurse differentiating germ cells during spermatogenesis,
534 and their function is modulated by metabolic (26, 56) and endocrine (34-36, 54)
535 factors, with significant impact on mature spermatozoa (49). Fat deposition in
536 the abdominal area, in humans, is correlated with poor sperm quality (15, 21),
537 likely due to increased testicular temperature (17, 24) and local inflammation
538 (32). In our previous work (12), we also reported reduced sperm quality which
539 was associated with fat deposition. Moreover, there is a decrease in the activity
540 of antioxidant enzymes (Cat and GSR) in the testes of life-long HFD fed mice.
541 Therefore, it is possible that extra lipid intake, notably in PUFAs, is the
542 cornerstone in testicular antioxidant balance. This hypothesis is supported by
543 the differences in lipid fractions between groups (Figure 4), the differences in
544 the correlations of lipid fractions against sperm parameters (Figure 6A), and the
545 sample separation achieved by the corresponding PCA (Figure 6B).
546 Nonetheless, more studies will be needed to confirm this hypothesis,
547 particularly by using a model in which HFD is replaced by a high-fat, low-PUFA
548 diet. Moreover, we have not considered the potential contamination of testicular
549 lipid profile by serum. Yet, testes were decapsulated before homogenization to
550 hinder this issue. Besides, the interference of serum lipid profile is unlikely
551 considering blood to testis volume (27) and a previous study comparing
552 testicular and serum lipid profiles (44).

553 HFD is the culprit for testicular lipid dysmetabolism. The proportion of SFAs is
554 the lowest in testes of mice from the HFD group, and the highest in testis from
555 mice of the CTRL group. Contrastingly, MUFA and PUFA fractions were more

556 abundant in HFD than in the CTRL group. As lard, one of the main components
557 of the diet formulations, is rich in oleic acid (18:1n9), it is not surprising that HFD
558 and HFDt testes are enriched in this fatty acid. Yet, the relative content of
559 MUFAs compared to PUFAs, in both groups, suggest that oleic acid and other
560 MUFAs are unsaturated into PUFAs. Besides, the detected n-3 and n-6 long-
561 chain PUFAs can only be synthesized after their precursors, the linoleic and
562 linolenic acid are obtained by diet, as they cannot be synthesized *de novo* in
563 mammals (39). According to Koeberle et al. (28), mammals store large amounts
564 of PUFAs in testes during puberty, by the action of the lysophosphatidic acid
565 acyltransferase 3, resulting in a unique FA profile. For instance,
566 docosapentaenoic acid (C22:5n-6, n-6 DPA) is more abundant in testis than in
567 other mammalian tissues (7, 74). Although several studies describe n-6 DPA-
568 enrichment in various tissues due to HFD (16, 43, 50), testicular content of DPA
569 was unchanged in our model, but we observed testicular enrichment in other n-
570 6 FAs (Table S5).

571 Regarding PUFAs, the n-3/n-6 ratio in testis supports an amelioration in
572 testicular metabolism after ceasing HFD feeding at early adulthood. The $\Delta 6$
573 desaturase (D6D) has been associated with the deleterious effects of HFD,
574 particularly regarding glucose resistance (23). The dietary n-3/n-6 ratio intake,
575 for humans, is ideally close to 1, and lower ratios (n-6 enrichment) are
576 associated with health deterioration including increased cardiovascular risk (59).
577 In human testis, a lower n-3/n-6 ratio has been reported in oligo and
578 asthenozoospermia (73). Herein, we found a much lower n-3/n-6 ratio (0.22) in
579 testicular FA content, in the CTRL group. Yet, this ratio was significantly lower
580 (0.18) in HFD-fed mice during their lifetime. Considering the critical role of

581 docosahexaenoic acid (C22:6n-3, DHA) in spermatogenesis, the detrimental
582 content of n-3 in testis may be associated with the observed phenotype, as it
583 cannot balance the pro-inflammatory environment induced by HFD. Effectively,
584 DHA supplementation was showed to improve testicular n-3/n-6 ratio,
585 concomitantly improving antioxidant balance (63). However, in our study, sperm
586 parameters did not correlate to the testicular n-3/n-6 ratio.

587 Although the HFD formulation had similar relative amounts of SFAs, MUFAs
588 and PUFAs comparing to the standard chow, the C18:3n-3/C18:2n-6 molar ratio
589 is an order of magnitude higher in HFD (according to the manufacturer
590 information). Interestingly, testicular cells responded to this difference by
591 accumulating even more n-6 PUFAs, without changing their n-3 PUFA content
592 (Figure 4/Table S5). Moreover, n-6 PUFA changes are distinguished not only by
593 an increase in the relative abundance of dietary available linoleic acid (C18:2n-
594 6) but also by an increase of dihomo- γ -linolenic acid (C20:3n-6), and
595 arachidonic acid (C20:4n-6, AA), which are obtained from linoleic acid by an
596 enzyme-catalyzed desaturation–elongation process. This may reflect an overall
597 inhibition of the D4Ds and D5D induced by HFD, notably by the relative
598 enrichment in the dietary n-3. D6D is considered the rate-limiting enzyme in the
599 desaturation-elongation processes in mammalian cells, but according to the
600 relative abundance of n-6 PUFAs to n-3 PUFAs, and the C20:4n-6/C18:2n-6
601 ratio, HFD does not change its activity nor it is overwhelmed by the extra dietary
602 n-3. Therefore, testicular metabolic pathways involving n-6 PUFA remodeling
603 and metabolism exhibit high sensitivity to the excess of dietary fat (Figure 4).

604 The structural importance of phospholipids and its FA composition to cell
605 membrane fluidity should not be overlooked (31). Testicular SFA content is

606 negatively correlated with bent neck defects, whilst positively correlated with
607 coiled tail defects. Interestingly, MUFAs present mirrored correlations. This
608 observation may be linked to the different membrane composition of the
609 midpiece (neck) and the tail, or even to different membrane lipid needs of germ
610 cells at different spermatogenic stages (70). However, due to the limited
611 availability of testicular samples, it was not possible to estimate the detailed
612 testicular content of neutral lipid and phospholipid classes, besides the total lipid
613 profile. In this context, it is noteworthy that FAs from the same lipid saturation
614 family can result in opposite outcomes in testicular function. DHA is reduced in
615 testes of acyl-CoA synthetase isoform 6 (ACSL6) KO mice, leading to an
616 enrichment in the AA (20). This change fosters a pro-inflammatory environment,
617 as AA is an n-6 PUFA and precursor of pro-inflammatory eicosanoids, whereas
618 DHA is an n-3 PUFA and precursor of resolvins. According to those authors,
619 ACSL6-KO mice suffered from subfertility, with hypogonadism,
620 oligozoospermia, reduced number of germ cells, and morphological
621 abnormalities of the seminiferous epithelium. Our data show that HFD group
622 presented overlapping phenotypes, such as AA accumulation in testes and
623 poorer sperm parameters, although without DHA depletion in testes, likely due
624 to its dietary intake. Particularly, testicular AA content is positively correlated to
625 sperm pin head defects. However, Hale et al. (20) further reported that DHA-
626 rich and AA-rich phospholipids are delocalized in testes of ACSL6-KO mice. So,
627 the relative testicular content in those FAs is crucial to maintain a normal
628 testicular ultrastructure and spermatogenesis although some caution must be
629 taken, as the characterization of FAs was not quantitative. Despite the different

630 proportions in lipid fractions between diet regimens, it is not possible to state
631 whether absolute testicular FA content is enriched after HFD.

632 HFD promotes a positive feedback towards a pro-inflammatory state in testis.
633 Both n-3/n-6 and C22:6n-3/C20:4n-6 reflect a shift towards pro-inflammatory
634 pathways in the testis of mice continuously fed by HFD (Table S5). Interestingly,
635 the same group presented lower CAT and GSR activity and lower potential to
636 prevent oxidative damage. The testicular enrichment in C18:1n-9, in HFD mice,
637 may promote cell membrane fluidity in testicular cells and, consequently, their
638 vulnerability to peroxidation and phospholipase A2. Ultimately, it leads to
639 increased release of PUFAs, particularly AA, a central precursor of pro-
640 inflammatory pathways (leukotrienes, thromboxanes and prostaglandins).
641 Overall, the present data indicate that HFD shifts the cellular redox environment
642 towards a more pro-oxidant and pro-inflammatory state, enhancing testes
643 susceptibility for oxidative stress and inflammatory processes development.
644 Thus, the absence of changes in lipid peroxidation (TBARS) and in the activity
645 of mitochondrial Electron-Transfer Chain activity complexes suggest that HFD
646 by itself seems not to be enough stimulus to trigger oxidative stress. It was
647 reported that HFD causes an increase in antioxidant metabolites in testis,
648 notably GSH and betaine (12). Although we cannot rule out that the decreased
649 activity of Cat and GSR can emerge from post-translational changes (e.g.
650 acetylation, phosphorylation and ubiquitination), it was reported that HFD has
651 not only a negative impact (decrease) on the expression of testicular antioxidant
652 enzymes (18, 32), but also promotes an increase in antioxidant metabolites in
653 testes, notably GSH and betaine (12). Thus, the increased testicular GSH and

654 betaine levels may be enough to keep the redox balance in testis despite the
655 decreased enzymatic antioxidant protection.

656 In addition to this, lipolysis can be another contributor to the observed
657 differences in lipid fractions, and a critical process to mediate membrane
658 integrity and fluidity of all cells in testicular tissue. It is well known that dietary
659 MUFAs promote lipolysis (48). Changes in testicular glycerol, choline, myo-
660 inositol and glycerophosphocholine in HFD (and partially in HFD_t) are likely due
661 to lipolysis and indicate increased phospholipid turnover and/or degradation.
662 Nevertheless, lipolysis raises another threat to seminiferous tubules stability.
663 Glycerol accumulates in the testes of HFD and HFD_t mice. Glycerol destabilizes
664 tight-junctions and desmosomes between SCs, causing a leaky blood-testis
665 barrier (10). We also observed an accumulation of the organic osmolytes
666 glycerophosphocholine and myo-inositol in testes, after HFD. Previously, we
667 reported an accumulation of betaine, glutamine and glutamate in the same
668 condition (12). Interestingly, this phenomenon has been previously reported in
669 kidney medullar cells, as a response against hypertonic stress (45). FA
670 oxidation requires a hydration step; therefore, the extra dietary intake of FAs
671 can induce hypertonic stress in testes, triggering this response in testicular
672 cells, notably SCs. Our data also suggests a protective effect of choline against
673 sperm tail defects. A recent study linked choline (and betaine) supplementation
674 with lipolysis activation, due to elevated succinate concentration (60) in plasma.
675 Interestingly, we have obtained opposite results in testes, after dietary
676 intervention (12). Yet, our data support a promotion of lipolysis in testes by HFD
677 in early adult life. Again, SCs are likely involved in this outcome, as their
678 metabolic activity has been described to be remodeled towards lipolysis as a

679 response to a high-energy environment, as it is the case of obesity (56). In our
680 model, we have observed that AMP and AMP/ATP ratio inversely correlated
681 with sperm head defects suggesting that energy-consuming pathways can be
682 beneficial to spermatozoa. Conversely, increased testicular energy charge
683 promoted sperm head defects. Additionally, sperm motility was reduced in
684 groups where our data suggest lipolysis overactivation (HFD and HFD_t groups)
685 as supported by the changes observed in metabolites related to phospholipids.
686 An exaggerated accumulation of lipid droplets in testis leads to lower sperm
687 motility, but a proper FA acid supply is needed for sperm capacitation in the
688 epididymis (37). Thus, different metabolic pathways related to different lipid
689 classes have different roles and importance not only in different testicular cells,
690 but also in different parts of the spermatozoon (66).

691 In sum, our data demonstrates that a HFD during early life akin to childhood
692 and puberty causes an excessive accumulation of unsaturated FAs in testes. A
693 diet intervention, replacing HFD for a balanced diet was proven effective in
694 protecting/preventing metabolic dysfunction. However, a HFD during early life
695 caused irreversible metabolic remodeling in testes, with long-term sperm
696 defects. Dietary intervention in early adulthood promotes lipolysis in testes,
697 particularly from unsaturated FAs, towards the CTRL state, but this process is
698 apparently too slow to recover normal sperm parameters. Mechanistically, our
699 data suggests that HFD promotes a pro-inflammatory state in testis, aggravated
700 by a positive feedback system that favors the accumulation of n-6 PUFAs,
701 precursors of inflammatory response signaling molecules. Our model did not
702 allow us to verify whether testicular lipid composition and normal sperm quality
703 could be achieved later in life, but we must also consider that sperm quality

704 declines with age, even in rodents (25). Epigenetic modifications are likely
705 involved in the observed phenotypes after HFD, especially those which have
706 not been reversed by diet switch. Indeed, the prepubertal period is critical for
707 epigenetic remodeling of germ cells (47, 58), and we plan to investigate the
708 influence those mechanisms in our model in future work. Our findings highlight
709 the importance of preventing childhood obesity, to avoid irreversible damage for
710 the reproductive health of the fathers of tomorrow, with unpredicted effects to
711 their progeny.

712

713 **Declaration of interest**

714 The authors declare no conflict of interest.

715

716 **Funding**

717 This work was supported by the Portuguese Foundation for Science and
718 Technology: L. Crisóstomo (SFRH/BD/128584/2017), M.G. Alves (IFCT2015
719 and PTDC/MEC-AND/28691/2017), P.F. Oliveira (IFCT2015), UMIB
720 (UID/Multi/00215/2019) and QOPNA (UID/QUI/00062/2019) co-funded by
721 FEDER funds (POCI/COMPETE 2020); by the Portuguese Society of
722 Diabetology: L. Crisóstomo and M.G. Alves (“Nuno Castel-Branco” research
723 grant and Group of Fundamental and Translational Research); and by the
724 Croatian Science Foundation: K. Starčević (IP-2016-06-3163).

725

726 **Author Contributions**

727 L.C., P.F.O., M.G.A. and R.L.B. contributed to study design, analysis and
728 interpretation of data. L.R., I.J., K.S., T.M., R.A.V. and L.C. performed
729 experimental work. L.C. edited the images and tables, performed the statistics
730 and contributed to the analysis and interpretation of data. R.L.B., J.F.R. and
731 R.A.V. critically reviewed the manuscript and suggested modifications. All the
732 authors contributed to manuscript writing/editing and approved the final version.

733

734 **Acknowledgments**

735 We acknowledge the Portuguese Nuclear Magnetic Resonance Network
736 (REDE/1517/RMN/2005) for access to their facilities. We thank Prof. Pedro N.
737 Oliveira (ICBAS-UP) for his advice on the statistical methods.

738

739 **Supplemental Data**

740 Supplemental tables S1 – S5 and the supplemental figure SF1 are available as

741 Supplemental Data:

742 URL: <https://figshare.com/s/785af8effa28e8bc2935>

743 DOI: <https://doi.org/10.6084/m9.figshare.12302171>

744

745

746 **REFERENCES**

- 747 1. **Allison DB, Paultre F, Maggio C, Mezzitis N, Pi-Sunyer FX.** The Use
748 of Areas Under Curves in Diabetes Research. *Diabetes Care* 18: 245-250,
749 1995.
- 750 2. **Alves MG, Oliveira PJ, Carvalho RA.** Substrate selection in hearts
751 subjected to ischemia/reperfusion: role of cardioplegic solutions and gender.
752 *NMR Biomed* 24: 1029-1037, 2011.
- 753 3. **Alves MG, Rato L, Carvalho RA, Moreira PI, Socorro S, Oliveira PF.**
754 Hormonal control of Sertoli cell metabolism regulates spermatogenesis. *Cell*
755 *Mol Life Sci* 70: 777-793, 2013.
- 756 4. **Antunes LC, Elkfury JL, Jornada MN, Foletto KC, Bertoluci MC.**
757 Validation of HOMA-IR in a model of insulin-resistance induced by a high-fat
758 diet in Wistar rats. *Arq Endocrinol Metabol* 60: 138-142, 2016.
- 759 5. **Avtanski D, Pavlov VA, Tracey KJ, Poretsky L.** Characterization of
760 inflammation and insulin resistance in high-fat diet-induced male C57BL/6J
761 mouse model of obesity. *Anim Models Exp Med* 2: 252-258, 2019.
- 762 6. **Bekaert M, Van Nieuwenhove Y, Calders P, Cuvelier CA, Batens A-H,**
763 **Kaufman J-M, Ouwens DM, Ruige JB.** Determinants of testosterone levels in
764 human male obesity. *Endocrine* 50: 202-211, 2015.
- 765 7. **Bieri JG, Prival EL.** Lipid composition of testes from various species.
766 *Comp Biochem Physiol* 15: 275-282, 1965.

- 767 8. **Borges BC, Garcia-Galiano D, da Silveira Cruz-Machado S, Han X,**
768 **Gavrulina GB, Saunders TL, Auchus RJ, Hammoud SS, Smith GD, Elias CF.**
769 Obesity-Induced Infertility in Male Mice Is Associated With Disruption of Crisp4
770 Expression and Sperm Fertilization Capacity. *Endocrinology* 158: 2930-2943,
771 2017.
- 772 9. **Caumo A, Perseghin G, Brunani A, Luzi L.** New Insights on the
773 Simultaneous Assessment of Insulin Sensitivity and β -Cell Function With the
774 HOMA2 Method. *Diabetes Care* 29: 2733-2734, 2006.
- 775 10. **Crisóstomo L, Alves MG, Calamita G, Sousa M, Oliveira PF.** Glycerol
776 and testicular activity: the good, the bad and the ugly. *Mol Hum Reprod* 23: 725-
777 737, 2017.
- 778 11. **Crisóstomo L, Alves MG, Gorga A, Sousa M, Riera MF, Galardo MN,**
779 **Meroni SB, Oliveira PF.** Molecular mechanisms and signalling pathways
780 involved in the nutritional support of spermatogenesis by Sertoli cells. In: *Sertoli*
781 *cells - Methods and Protocols* (1st ed.), edited by Alves MG and Oliveira PF.
782 New York, USA: Humana Press, 2018, p. 129-155.
- 783 12. **Crisóstomo L, Rato L, Jarak I, Silva BM, Raposo JF, Batterham RL,**
784 **Oliveira PF, Alves MG.** A switch from high-fat to normal diet does not restore
785 sperm quality but prevents metabolic syndrome. *Reproduction* 158: 377-387,
786 2019.
- 787 13. **del Río LA, Ortega MG, López AL, Gorgé JL.** A more sensitive
788 modification of the catalase assay with the Clark oxygen electrode: application
789 to the kinetic study of the pea leaf enzyme. *Anal Biochem* 80: 409-415, 1977.

- 790 14. **Eisenberg ML, Sundaram R, Maisog J, Buck Louis GM.** Diabetes,
791 medical comorbidities and couple fecundity. *Hum Reprod* 31: 2369-2376, 2016.
- 792 15. **Faure C, Dupont C, Baraibar MA, Ladouce R, Cedrin-Durnerin I, Wolf**
793 **JP, Lévy R.** In Subfertile Couple, Abdominal Fat Loss in Men Is Associated with
794 Improvement of Sperm Quality and Pregnancy: A Case-Series. *PLoS one* 9:
795 e86300, 2014.
- 796 16. **Garg ML, Sebokova E, Thomson ABR, Clandinin MT.** Δ 6-desaturase
797 activity in liver microsomes of rats fed diets enriched with cholesterol and/or ω 3
798 fatty acids. *Biochem J* 249: 351-356, 1988.
- 799 17. **Garolla A, Torino M, Miola P, Caretta N, Pizzol D, Menegazzo M,**
800 **Bertoldo A, Foresta C.** Twenty-four-hour monitoring of scrotal temperature in
801 obese men and men with a varicocele as a mirror of spermatogenic function.
802 *Hum Reprod* 30: 1006-1013, 2015.
- 803 18. **Ghosh S, Mukherjee S.** Testicular germ cell apoptosis and sperm
804 defects in mice upon long-term high fat diet feeding. *J Cell Physiol* 233: 6896-
805 6909, 2018.
- 806 19. **Guo D, Wu W, Tang Q, Qiao S, Chen Y, Chen M, Teng M, Lu C, Ding**
807 **H, Xia Y, Hu L, Chen D, Sha J, Wang X.** The impact of BMI on sperm
808 parameters and the metabolite changes of seminal plasma concomitantly.
809 *Oncotarget* 8: 48619-48634, 2017.
- 810 20. **Hale BJ, Fernandez RF, Kim SQ, Diaz VD, Jackson SN, Liu L, Brenna**
811 **JT, Hermann BP, Geyer CB, Ellis JM.** Acyl-CoA Synthetase 6 enriches

812 seminiferous tubules with the omega-3 fatty acid DHA and is required for male
813 fertility in the mouse. *J Biol Chem* 234: 14394-14405, 2019.

814 21. **Hammoud AO, Gibson M, Peterson CM, Meikle AW, Carrell DT.**
815 Impact of male obesity on infertility: a critical review of the current literature.
816 *Fertil Steril* 90: 897-904, 2008.

817 22. **Hruby A, Manson JE, Qi L, Malik VS, Rimm EB, Sun Q, Willett WC,**
818 **Hu FB.** Determinants and Consequences of Obesity. *Am J Public Health* 106:
819 1656-1662, 2016.

820 23. **Hucik B, Sarr O, Nakamura MT, Dyck DJ, Mutch DM.** Reduced delta-6
821 desaturase activity partially protects against high-fat diet-induced impairment in
822 whole-body glucose tolerance. *J Nutr Biochem* 67: 173-181, 2019.

823 24. **Ivell R.** Lifestyle impact and the biology of the human scrotum. *Reprod*
824 *Biol Endocrin* 5: 15, 2007.

825 25. **Jarak I, Almeida S, Carvalho RA, Sousa M, Barros A, Alves MG,**
826 **Oliveira PF.** Senescence and declining reproductive potential: Insight into
827 molecular mechanisms through testicular metabolomics. *BBA - Mol Basis Dis*
828 1864: 3388-3396, 2018.

829 26. **Jesus TT, Oliveira PF, Silva J, Barros A, Ferreira R, Sousa M, Cheng**
830 **CY, Silva BM, Alves MG.** Mammalian target of rapamycin controls glucose
831 consumption and redox balance in human Sertoli cells. *Fertil Steril* 105: 825-
832 833.e823, 2016.

- 833 27. **Kaliss N, Pressman D.** Plasma and Blood Volumes of Mouse Organs,
834 As Determined with Radioactive Iodoproteins. *Proceedings of the Society for*
835 *Experimental Biology and Medicine* 75: 16-20, 1950.
- 836 28. **Koeberle A, Shindou H, Harayama T, Yuki K, Shimizu T.**
837 Polyunsaturated fatty acids are incorporated into maturing male mouse germ
838 cells by lysophosphatidic acid acyltransferase 3. *FASEB J* 26: 169-180, 2012.
- 839 29. **Kvist U, Björndahl L, Nordic Association for Andrology, European**
840 **Society of Human Reproduction and Embryology, Andrology Special**
841 **Interest Group.** *Manual on basic semen analysis: 2002.* Oxford: Published in
842 association with ESHRE by Oxford University Press, 2002.
- 843 30. **Levy JC, Matthews DR, Hermans MP.** Correct Homeostasis Model
844 Assessment (HOMA) Evaluation Uses the Computer Program. *Diabetes Care*
845 21: 2191-2192, 1998.
- 846 31. **Lingwood D, Simons K.** Lipid Rafts As a Membrane-Organizing
847 Principle. *Science* 327: 46-50, 2010.
- 848 32. **Liu G-L, Zhang Y-M, Dai D-Z, Ding M-J, Cong X-D, Dai Y.** Male
849 hypogonadism induced by high fat diet and low dose streptozotocin is mediated
850 by activated endoplasmic reticulum stress and I κ B β and attenuated by argirein
851 and valsartan. *Eur J Pharmacol* 713: 78-88, 2013.
- 852 33. **Llewellyn A, Simmonds M, Owen CG, Woolacott N.** Childhood obesity
853 as a predictor of morbidity in adulthood: a systematic review and meta-analysis.
854 *Obes Rev* 17: 56-67, 2016.

- 855 34. **Martins AD, Monteiro MP, Silva BM, Barros A, Sousa M, Carvalho**
856 **RA, Oliveira PF, Alves MG.** Metabolic dynamics of human Sertoli cells are
857 differentially modulated by physiological and pharmacological concentrations of
858 GLP-1. *Toxicol Appl Pharmacol* 362: 1-8, 2019.
- 859 35. **Martins AD, Moreira AC, Sá R, Monteiro MP, Sousa M, Carvalho RA,**
860 **Silva BM, Oliveira PF, Alves MG.** Leptin modulates human Sertoli cells
861 acetate production and glycolytic profile: a novel mechanism of obesity-induced
862 male infertility? *BBA - Mol Basis Dis* 1852: 1824-1832, 2015.
- 863 36. **Martins AD, Sá R, Monteiro MP, Barros A, Sousa M, Carvalho RA,**
864 **Silva BM, Oliveira PF, Alves MG.** Ghrelin acts as energy status sensor of male
865 reproduction by modulating Sertoli cells glycolytic metabolism and mitochondrial
866 bioenergetics. *Mol Cell Endocrinol* 434: 199-209, 2016.
- 867 37. **Masaki H, Kim N, Nakamura H, Kumasawa K, Kamata E, Hirano K-i,**
868 **Kimura T.** Long-chain fatty acid triglyceride (TG) metabolism disorder impairs
869 male fertility: a study using adipose triglyceride lipase deficient mice. *Mol Hum*
870 *Reprod* 23: 452-460, 2017.
- 871 38. **Mendes D, Oliveira MM, Moreira PI, Coutinho J, Nunes FM, Pereira**
872 **DM, Valentão P, Andrade PB, Videira RA.** Beneficial effects of white wine
873 polyphenols-enriched diet on Alzheimer's disease-like pathology. *J Nutr*
874 *Biochem* 55: 165-177, 2018.
- 875 39. **Miyazaki M, Ntambi JM.** Fatty acid desaturation and chain elongation in
876 mammals. In: *Biochemistry of Lipids, Lipoproteins and Membranes* (5th ed.),

877 edited by Vance DE and Vance JE. San Diego, USA: Elsevier, 2008, p. 191-
878 211.

879 40. **Monteiro-Cardoso VF, Oliveira MM, Melo T, Domingues MR, Moreira**
880 **PI, Ferreira E, Peixoto F, Videira RA.** Cardiolipin profile changes are
881 associated to the early synaptic mitochondrial dysfunction in Alzheimer's
882 disease. *J Alzheimers Dis* 43: 1375-1392, 2015.

883 41. **Muecke L, Simons-Morton B, Huang IW, Parcel G.** Is Childhood
884 Obesity Associated with High-Fat Foods and Low Physical Activity? *J Sch*
885 *Health* 62: 19-23, 1992.

886 42. **Mulholland J, Mallidis C, Agbaje I, McClure N.** Male diabetes mellitus
887 and assisted reproduction treatment outcome. *Reprod Biomed Online* 22: 215-
888 219, 2011.

889 43. **Naoe S, Tsugawa H, Takahashi M, Ikeda K, Arita M.** Characterization
890 of lipid profiles after dietary intake of polyunsaturated fatty acids using
891 integrated untargeted and targeted lipidomics. *Metabolites* 9: 241, 2019.

892 44. **Napoli JL, McCormick AM.** Tissue dependence of retinoic acid
893 metabolism in vivo. *Biochimica et Biophysica Acta (BBA) - Lipids and Lipid*
894 *Metabolism* 666: 165-175, 1981.

895 45. **Neuhofer W, Beck F-X.** Response of renal medullary cells to osmotic
896 stress. In: *Cellular Stress Responses in Renal Diseases* (1st ed.), edited by
897 Razzaque MS and Taguchi T. Basel, Switzerland: Karger Publishers, 2005, p.
898 21-34.

- 899 46. **Neves D, Valentão P, Bernardo J, Oliveira MC, Ferreira JMG, Pereira**
900 **DM, Andrade PB, Videira RA.** A new insight on elderberry anthocyanins
901 bioactivity: Modulation of mitochondrial redox chain functionality and cell redox
902 state. *J Funct Foods* 56: 145-155, 2019.
- 903 47. **Nilsson EE, Sadler-Riggelman I, Skinner MK.** Environmentally induced
904 epigenetic transgenerational inheritance of disease. *Environmental Epigenetics*
905 4, 2018.
- 906 48. **O'Connor S, Rudkowska I.** Dietary Fatty Acids and the Metabolic
907 Syndrome: A Personalized Nutrition Approach. In: *Advances in Food and*
908 *Nutrition Research* (1st ed.), edited by Toldrá F. Oxford, UK: Academic Press,
909 2019, p. 43-146.
- 910 49. **Oliveira PF, Sousa M, Silva BM, Monteiro MP, Alves MG.** Obesity,
911 energy balance and spermatogenesis. *Reproduction* 153: R173-R185, 2017.
- 912 50. **Ostermann AI, Waindok P, Schmidt MJ, Chiu C-Y, Smyl C, Rohwer**
913 **N, Weylandt K-H, Schebb NH.** Modulation of the endogenous omega-3 fatty
914 acid and oxylipin profile in vivo—A comparison of the fat-1 transgenic mouse
915 with C57BL/6 wildtype mice on an omega-3 fatty acid enriched diet. *PLoS one*
916 12, 2017.
- 917 51. **Palmer NO, Bakos HW, Fullston T, Lane M.** Impact of obesity on male
918 fertility, sperm function and molecular composition. *Spermatogenesis* 2: 253-
919 263, 2012.
- 920 52. **Rastrelli G, O'Neill TW, Ahern T, Bártfai G, Casanueva FF, Forti G,**
921 **Keevil B, Giwercman A, Han TS, Slowikowska-Hilczer J, Lean MEJ,**

922 **Pendleton N, Punab M, Antonio L, Tournoy J, Vanderschueren D, Maggi M,**
923 **Huhtaniemi IT, Wu FCW, group tEs.** Symptomatic androgen deficiency
924 develops only when both total and free testosterone decline in obese men who
925 may have incident biochemical secondary hypogonadism: Prospective results
926 from the EMAS. *Clin Endocrinol* 89: 459-469, 2018.

927 53. **Rato L, Alves MG, Dias TR, Lopes G, Cavaco JE, Socorro S, Oliveira**
928 **PF.** High-energy diets may induce a pre-diabetic state altering testicular
929 glycolytic metabolic profile and male reproductive parameters. *Andrology* 1:
930 495-504, 2013.

931 54. **Rato L, Alves MG, Duarte AI, Santos MS, Moreira PI, Cavaco JE,**
932 **Oliveira PF.** Testosterone deficiency induced by progressive stages of diabetes
933 mellitus impairs glucose metabolism and favors glycogenesis in mature rat
934 Sertoli cells. *Int J Biochem Cell Biol* 66: 1-10, 2015.

935 55. **Rato L, Alves MG, Socorro S, Duarte AI, Cavaco JE, Oliveira PF.**
936 Metabolic regulation is important for spermatogenesis. *Nat Rev Urol* 9: 330-338,
937 2012.

938 56. **Rato L, Duarte AI, Tomás GD, Santos MS, Moreira PI, Socorro S,**
939 **Cavaco JE, Alves MG, Oliveira PF.** Pre-diabetes alters testicular PGC1-
940 α /SIRT3 axis modulating mitochondrial bioenergetics and oxidative stress. *BBA*
941 - *Bioenergetics* 1837: 335-344, 2014.

942 57. **Roqueta-Rivera M, Stroud CK, Haschek WM, Akare SJ, Segre M,**
943 **Brush RS, Agbaga M-P, Anderson RE, Hess RA, Nakamura MT.**
944 Docosahexaenoic acid supplementation fully restores fertility and

945 spermatogenesis in male delta-6 desaturase-null mice. *J Lipid Res* 51: 360-367,
946 2010.

947 58. **Schagdarsurengin U, Steger K.** Epigenetics in male reproduction:
948 effect of paternal diet on sperm quality and offspring health. *Nat Rev Urol* 13:
949 584, 2016.

950 59. **Simopoulos AP.** The importance of the ratio of omega-6/omega-3
951 essential fatty acids. *Biomed Pharmacother* 56: 365-379, 2002.

952 60. **Sivanesan S, Taylor A, Zhang J, Bakovic M.** Betaine and Choline
953 Improve Lipid Homeostasis in Obesity by Participation in Mitochondrial
954 Oxidative Demethylation. *Front Nutr* 5: 00061, 2018.

955 61. **Smith PK, Krohn RI, Hermanson GT, Mallia AK, Gartner FH,
956 Provenzano MD, Fujimoto EK, Goeke NM, Olson BJ, Klenk DC.**
957 Measurement of protein using bicinchoninic acid. *Anal Biochem* 150: 76-85,
958 1985.

959 62. **Stanford KI, Rasmussen M, Baer LA, Lehnig AC, Rowland LA, White
960 JD, So K, De Sousa-Coelho AL, Hirshman MF, Patti M-E, Rando OJ,
961 Goodyear LJ.** Paternal Exercise Improves Glucose Metabolism in Adult
962 Offspring. *Diabetes* 67: 2530-2540, 2018.

963 63. **Starčević K, Maurić M, Galan A, Gudan Kurilj A, Mašek T.** Effects of
964 different n6/n3 ratios and supplementation with DHA and EPA on the testicular
965 histology and lipogenesis in streptozotocin-treated rats. *Andrologia* 50: e13067,
966 2018.

- 967 64. **Stokes VJ, Anderson RA, George JT.** How does obesity affect fertility
968 in men – and what are the treatment options? *Clin Endocrinol* 82: 633-638,
969 2015.
- 970 65. **Sumner LW, Amberg A, Barrett D, Beale MH, Beger R, Daykin CA,**
971 **Fan TWM, Fiehn O, Goodacre R, Griffin JL, Hankemeier T, Hardy N, Harnly**
972 **J, Higashi R, Kopka J, Lane AN, Lindon JC, Marriott P, Nicholls AW, Reily**
973 **MD, Thaden JJ, Viant MR.** Proposed minimum reporting standards for
974 chemical analysis: Chemical Analysis Working Group (CAWG) Metabolomics
975 Standards Initiative (MSI). *Metabolomics* 3: 211-221, 2007.
- 976 66. **Takei GL, Miyashiro D, Mukai C, Okuno M.** Glycolysis plays an
977 important role in energy transfer from the base to the distal end of the flagellum
978 in mouse sperm. *J Exp Biol* 217: 1876-1886, 2014.
- 979 67. **Taylor R.** Interpretation of the Correlation Coefficient: A Basic Review. *J*
980 *Diagn Med Sonogr* 6: 35-39, 1990.
- 981 68. **Wallace TM, Levy JC, Matthews DR.** Use and Abuse of HOMA
982 Modeling. *Diabetes Care* 27: 1487-1495, 2004.
- 983 69. **Wishart DS, Tzur D, Knox C, Eisner R, Guo AC, Young N, Cheng D,**
984 **Jewell K, Arndt D, Sawhney S, Fung C, Nikolai L, Lewis M, Coutouly MA,**
985 **Forsythe I, Tang P, Shrivastava S, Jeroncic K, Stothard P, Amegbey G,**
986 **Block D, Hau DD, Wagner J, Miniaci J, Clements M, Gebremedhin M, Guo**
987 **N, Zhang Y, Duggan GE, MacInnis GD, Weljie AM, Dowlatabadi R,**
988 **Bamforth F, Clive D, Greiner R, Li L, Marrie T, Sykes BD, Vogel HJ,**

989 **Querengesser L.** HMDB: The human metabolome database. *Nucleic Acids*
990 *Res* 35: D521-D526, 2007.

991 70. **Wolf DE, Scott BK, Millette CF.** The development of regionalized lipid
992 diffusibility in the germ cell plasma membrane during spermatogenesis in the
993 mouse. *J Cell Biol* 103: 1745-1750, 1986.

994 71. **World Health Organization.** *Global status report on noncommunicable*
995 *diseases 2014*. Geneva, Switzerland: WHO Press, 2014.

996 72. **World Health Organization.** *Obesity: preventing and managing the*
997 *global epidemic*. Genève: World Health Organization, 2000.

998 73. **Zalata AA, Christophe AB, Depuydt CE, Schoonjans F, Comhaire**
999 **FH.** The fatty acid composition of phospholipids of spermatozoa from infertile
1000 patients. *Mol Hum Reprod* 4: 111-118, 1998.

1001 74. **Zanetti SR, Maldonado EN, Aveldaño MI.** Doxorubicin Affects
1002 Testicular Lipids with Long-Chain (C₁₈-C₂₂) and Very Long-Chain (C₂₄-C₃₂)
1003 Polyunsaturated Fatty Acids. *Cancer res* 67: 6973-6980, 2007.

1004

1005

1006

1007

1008 **FIGURE LEGENDS**

1009 **Figure 1:** HOMA2 indexes and Disposition Index of mice fed standard chow
1010 (CTRL) or life-long high-fat diet (HFD) or subjected to diet correction after 60
1011 days (HFD_t). Fasting glycemia and insulin were used as inputs for the iHOMA2
1012 calculator (University of Oxford, UK). Results are expressed as Tukey's whisker
1013 boxes (median, 25th to 75th percentiles ± 1.5 IQR). Extreme values are
1014 represented individually (● CTRL – standard chow; ■ HFD – high-fat diet; ▲
1015 HFD_t – transient high-fat diet). Data was tested by one-way ANOVA with
1016 Tukey's HSD for group comparison. Significance was considered when $p <$
1017 0.05. † group average; * vs. CTRL; # vs. HFD. * $p < 0.05$; ** $p < 0.01$; *** $p < 0.001$;
1018 **** $p < 0.0001$.

1019

1020 **Figure 2:** Epididymal sperm parameters of mice fed standard chow (CTRL) or
1021 life-long high-fat diet (HFD) or subjected to diet correction after 60 days (HFD_t).
1022 Results are expressed as mean ± standard deviation. Sperm count is expressed
1023 as million spermatozoa per milliliter (M/mL), while other parameters are
1024 expressed as the % of total sperm cells. Individual values are represented (●
1025 CTRL – standard chow; ■ HFD – high-fat diet; ▲ HFD_t – transient high-fat diet).
1026 Data was tested by one-way ANOVA with Tukey's HSD for group comparison.
1027 Significance was considered when $p < 0.05$. * vs. CTRL; # vs. HFD. * $p < 0.05$; **
1028 $p < 0.01$; *** $p < 0.001$; **** $p < 0.0001$.

1029

1030 **Figure 3:** Lipid peroxidation (TBARS assay) and activity of the four main
1031 enzymes of the antioxidative defense metabolism – SOD, GSR, GPx and CAT

1032 in the testis of mice standard chow (CTRL) or life-long high-fat diet (HFD) or
1033 subjected to diet correction after 60 days (HFD_t). Two outliers were excluded
1034 from the analysis resulting in n=5 for every group. Results are expressed as
1035 Tukey's whisker boxes (median, 25th to 75th percentiles ± 1.5 IQR). Data was
1036 tested by one-way ANOVA with Tukey's HSD for group comparisons.
1037 Significance was considered when p < 0.05. ⁺ group average; * vs. CTRL; # vs.
1038 HFD. * p<0.05; ** p<0.01; *** p<0.001; **** p<0.0001.

1039

1040 **Figure 4:** Relative abundance of lipids in the apolar fraction of testicular
1041 extracts of mice fed standard chow (CTRL) or life-long high-fat diet (HFD) or
1042 subjected to diet correction after 60 days (HFD_t), grouped by saturation. CTRL –
1043 standard chow; HFD – high-fat diet; HFD_t – transient high-fat diet. The results
1044 were tested by one-way ANOVA with Tukey's Honest Significance Difference
1045 (HSD) for post-hoc group comparisons. Significance was considered when p <
1046 0.05. * vs. CTRL; # vs. HFD. * p<0.05; ** p<0.01; *** p<0.001; **** p<0.0001.
1047 Abbreviations: SFA – Saturated Fatty Acids; MUFAs – Monounsaturated Fatty
1048 Acids; PUFAs – Polyunsaturated Fatty Acids.

1049

1050 **Figure 5:** Correlations between sperm parameters to endocrine, antioxidant,
1051 mitochondrial and bioenergetic parameters. **A)** Individual scores for the
1052 previously assessed parameters were correlated using the parametric Pearson
1053 correlation (n = 24). Values are represented as Pearson r coefficients,
1054 according to the color scale, when p < 0.05. **B)** Sample distribution according to
1055 2PCs extracted by PCA, and based on correlations between sperm parameters

1056 to endocrine, antioxidant, mitochondrial and bioenergetic parameters (n = 10).
1057 ^aAfter base-10 logarithmic transformation. Abbreviations: CS – Citrate
1058 Synthase; C I – Complex I activity; C II - Complex II activity; C IV - Complex IV
1059 activity; C V - Complex V activity; Pool – Total adenosine nucleotide pool;
1060 Glycaemia – Fasting glycemia; FSH – Serum FSH; LH – Serum LH; E₂ – Serum
1061 17β-estradiol; T – Serum testosterone; TBARS – Thiobarbituric Acid reactive
1062 species assay (Lipid peroxidation); SOD – Superoxide dismutase activity; GPx
1063 – Glutathione Peroxidase activity; CAT – Catalase activity; GSR – Glutathione-
1064 disulphide Reductase activity.

1065

1066 **Figure 6:** Correlation of sperm parameters to testicular lipids and lipid
1067 precursors. **A)** Individual scores for the previously assessed parameters were
1068 correlated using the parametric Pearson correlation (n = 14). Values are
1069 represented as Pearson r coefficients, according to the color scale, when p <
1070 0.05. * p<0.05; ** p<0.01; *** p<0.001; **** p<0.0001. **B)** Sample distribution
1071 according to 2PCs extracted by PCA, and based on correlations between sperm
1072 parameters to testicular lipids and lipid precursors (n = 11). ^a Spearman rho
1073 coefficients, as the normality assumption was violated for this variable.
1074 Abbreviations: EtAmine – Ethanolamine; PhosEtAmine –
1075 Phosphoethanolamine; 3OH-But – 3'-hydroxybutyrate; PhosCholine –
1076 Phosphocholine; GlyPhosCholine – Glycerophosphocholine; SFAs – Saturated
1077 Fatty Acids; MUFAs – Monounsaturated Fatty Acids; PUFAs – Polyunsaturated
1078 Fatty Acids.

1079

1080 **SUPPLEMENTAL DATA**

1081 **Table S1:** ¹H NMR resonance assignment of polar testicular lipid precursors (s:
1082 singlet, d: doublet, dd: doublet of doublets, t: triplet, m: multiplet).

1083

1084 **Table S2:** Reproductive parameters. Results are expressed as the mean (%) ±
1085 standard error of the mean. Data tested using χ^2 test, based on the number of
1086 successful matings to the number of attempts (success rate), and on the
1087 number of male offspring to the litter size (male pups).

1088

1089 **Table S3:** Enzymatic activity of mitochondrial complexes in testes of mice fed
1090 standard chow (CTRL), life-long high-fat diet (HFD), and those subjected to diet
1091 correction after 60 days (HFD_t). Results are expressed as mean ± standard
1092 deviation. Experimental groups were compared by one-way ANOVA with
1093 Tukey's HSD. Significance was considered when $p < 0.05$. * vs. CTRL; # vs.
1094 HFD. * $p < 0.05$; ** $p < 0.01$; *** $p < 0.001$; **** $p < 0.0001$.

1095

1096 **Table S4:** Testicular bioenergetics of mice fed standard chow (CTRL), life-long
1097 high-fat diet (HFD), and those subjected to diet correction after 60 days (HFD_t).
1098 Results are expressed as mean ± standard deviation. Experimental groups
1099 were compared by one-way ANOVA with Tukey's HSD. Significance was
1100 considered when $p < 0.05$. * vs. CTRL; # vs. HFD. * $p < 0.05$; ** $p < 0.01$; *** $p <$
1101 0.001 ; **** $p < 0.0001$.

1102

1103

1104 **Table S5:** Fatty acid composition of the apolar testicular extracts of mice fed
1105 standard chow (CTRL), life-long high-fat diet (HFD), and those subjected to diet
1106 correction after 60 days (HFD_t). FAs are presented as: Common name (Lipid
1107 numbers). Results are expressed as the mean (% of total lipids) ± standard
1108 deviation. Results were tested by one-way ANOVA with Tukey's HSD.
1109 Significance was considered when $p < 0.05$. * vs. CTRL; # vs. HFD. * $p < 0.05$; **
1110 $p < 0.01$; *** $p < 0.001$; **** $p < 0.0001$. Abbreviations: SFAs – Saturated Fatty
1111 Acids; MUFAs – Monounsaturated Fatty Acids; PUFAs – Polyunsaturated Fatty
1112 Acids.

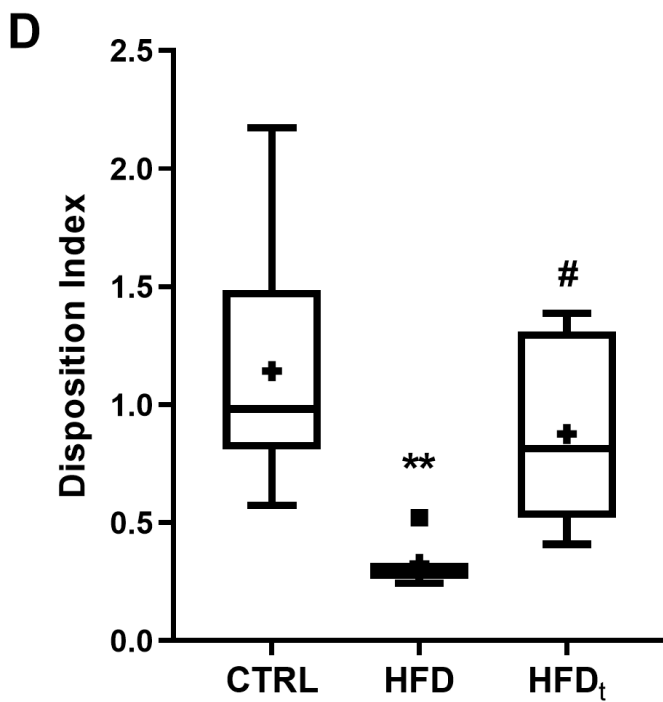
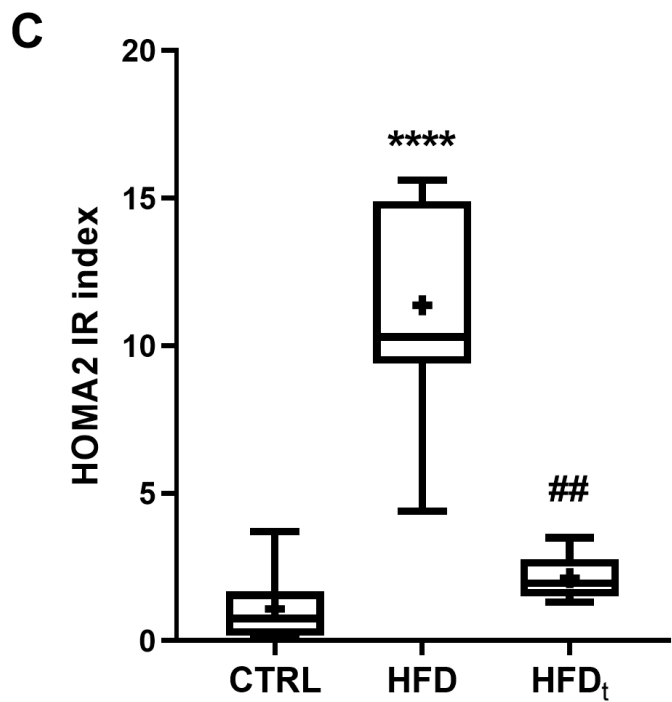
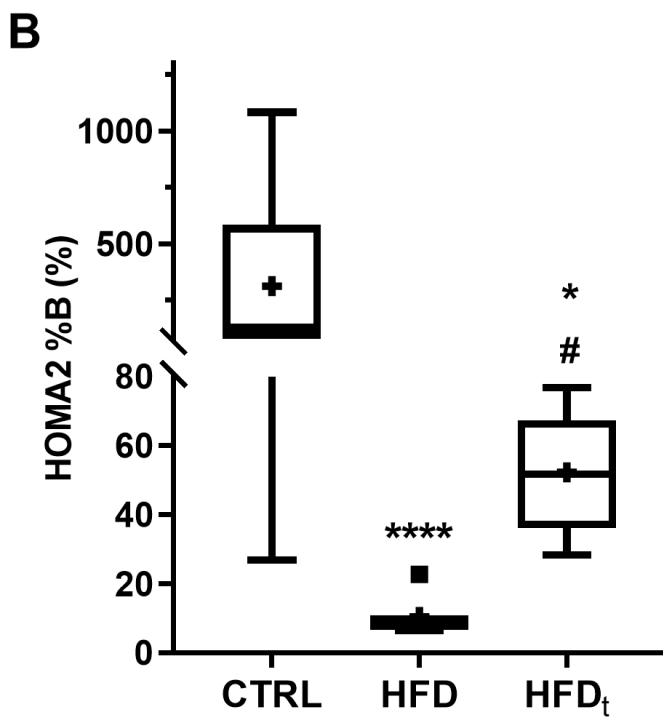
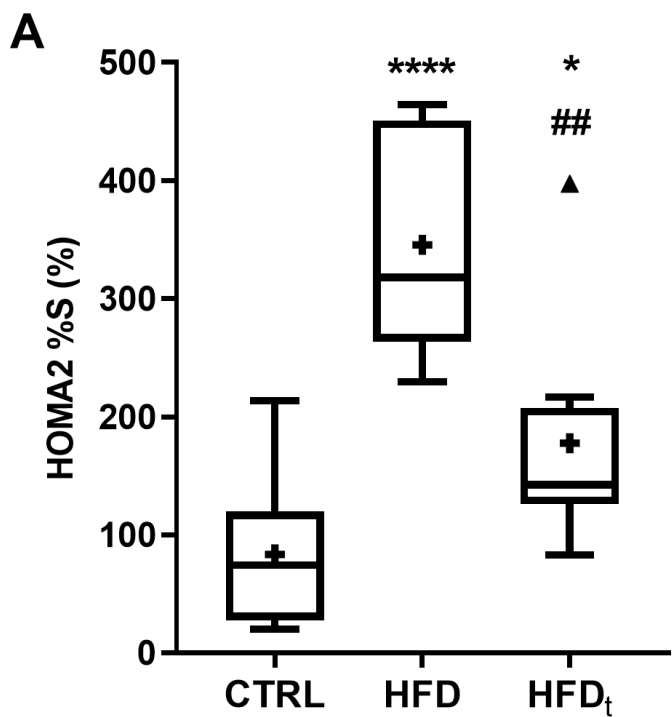
1113

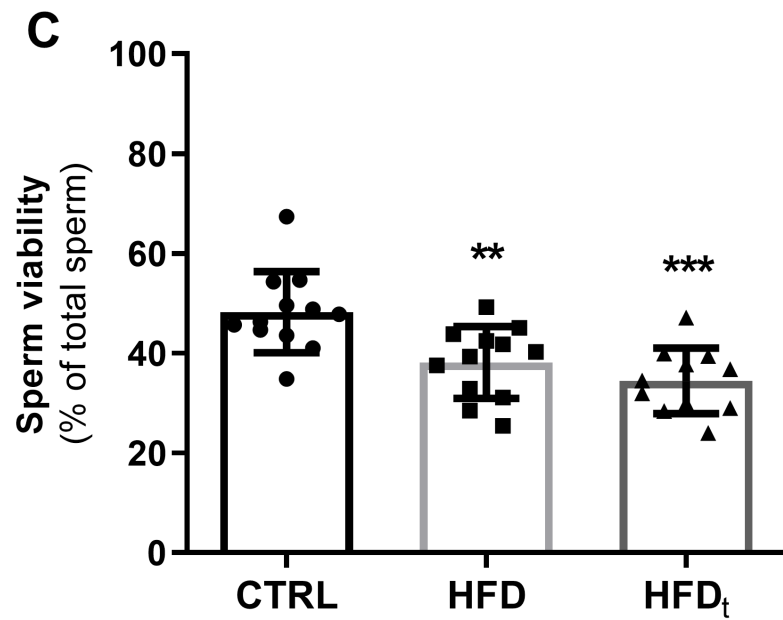
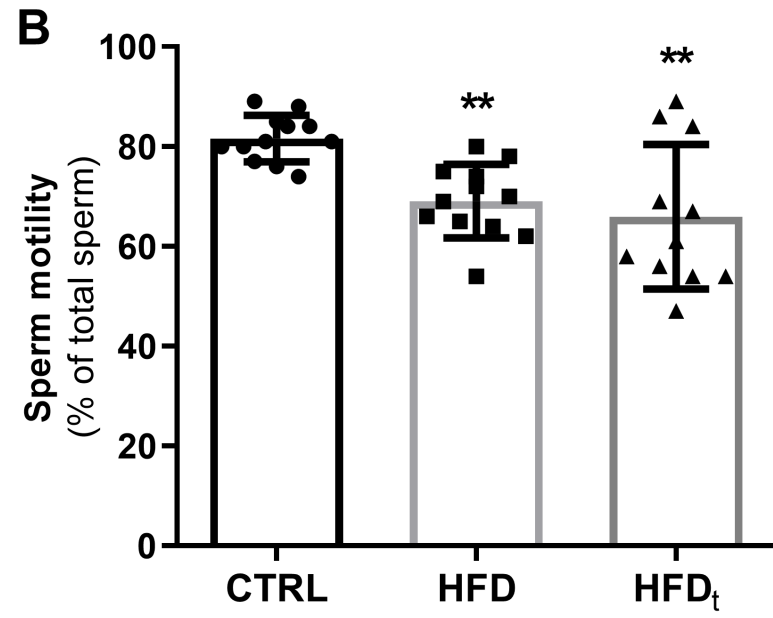
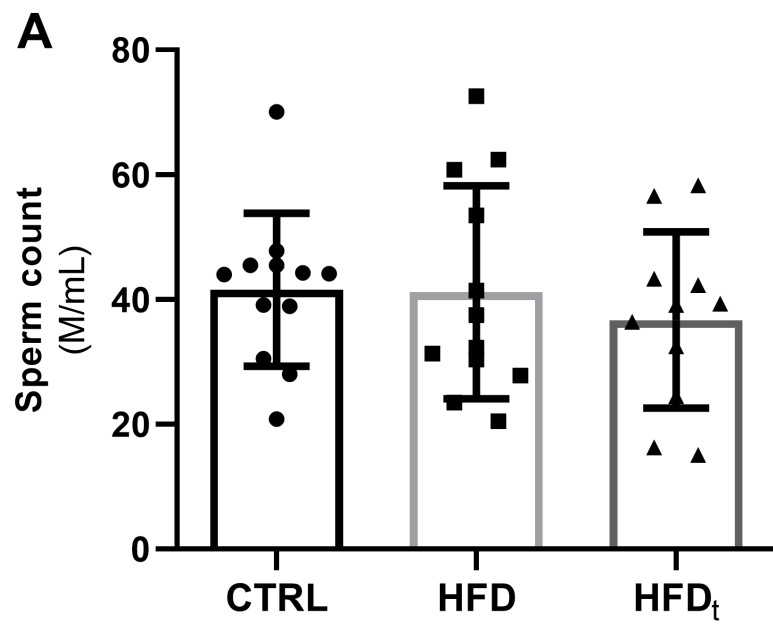
1114 **Figure SF1:** Body weight and food/water intake monitoring throughout the
1115 experiment. A) Average body weight 60 days after weaning, when diet reversion
1116 was performed to HFD_t group. B) Average body weight at the end of the
1117 experiment, 200 days after weaning. C) Cumulative food intake per mouse. D)
1118 Cumulative water intake per mouse. Results are expressed as mean ± standard
1119 deviation. Data were tested using one-way ANOVA corrected by Tukey's HSD.
1120 Significance was considered when $p < 0.05$. * vs. CTRL; # vs. HFD. * $p < 0.05$;
1121 ** $p < 0.01$; *** $p < 0.001$; **** $p < 0.0001$.

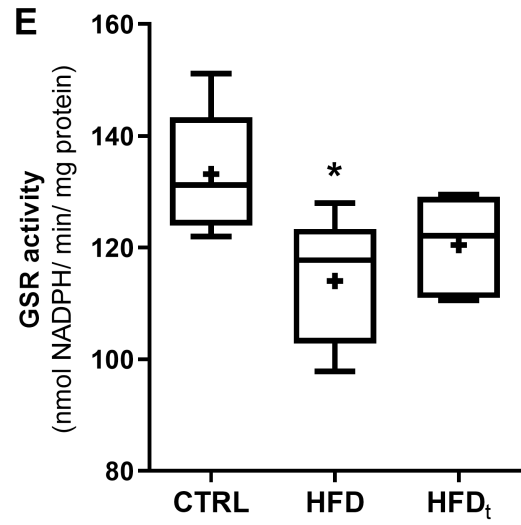
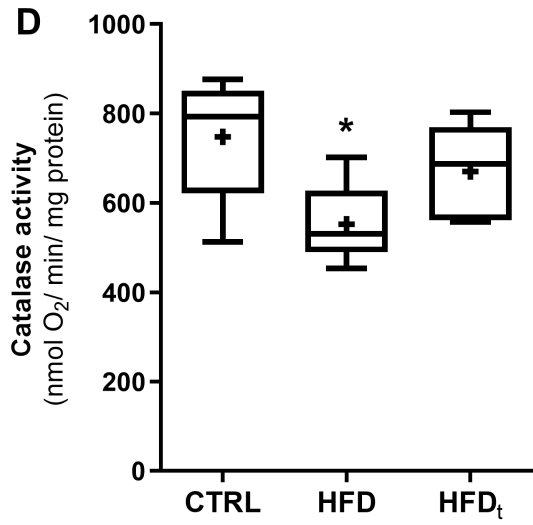
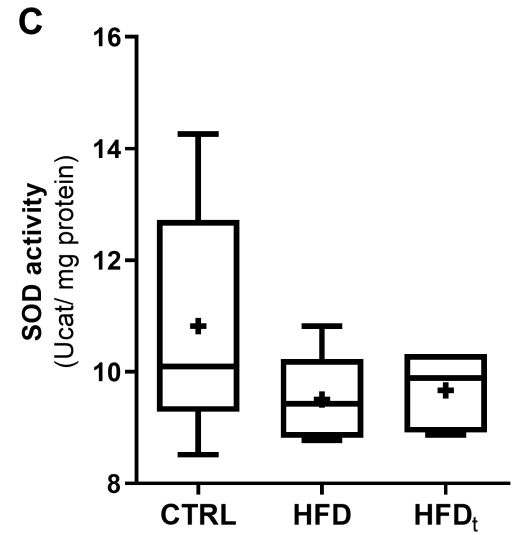
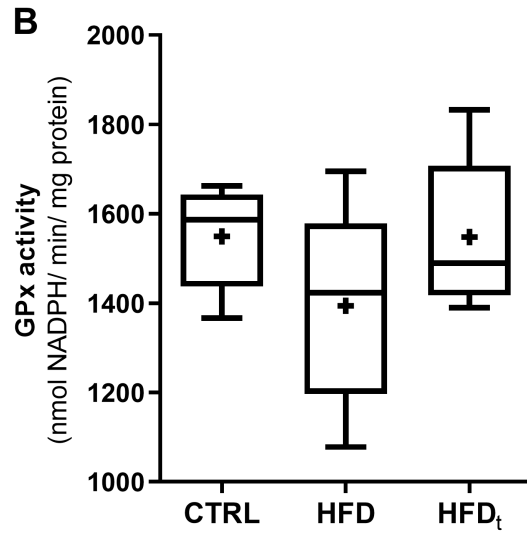
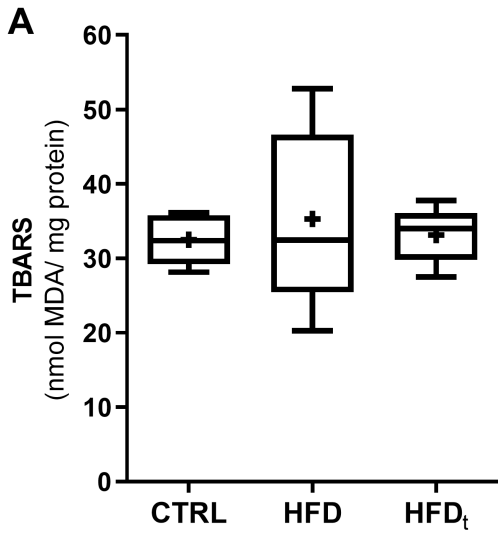
1122

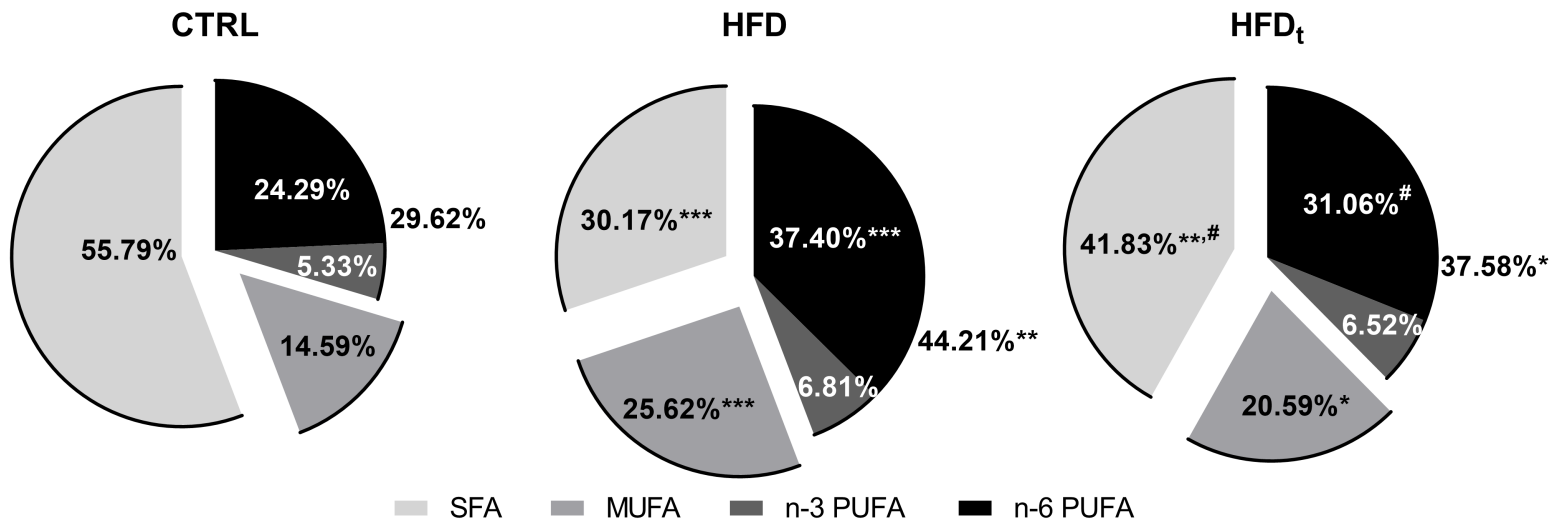
1123

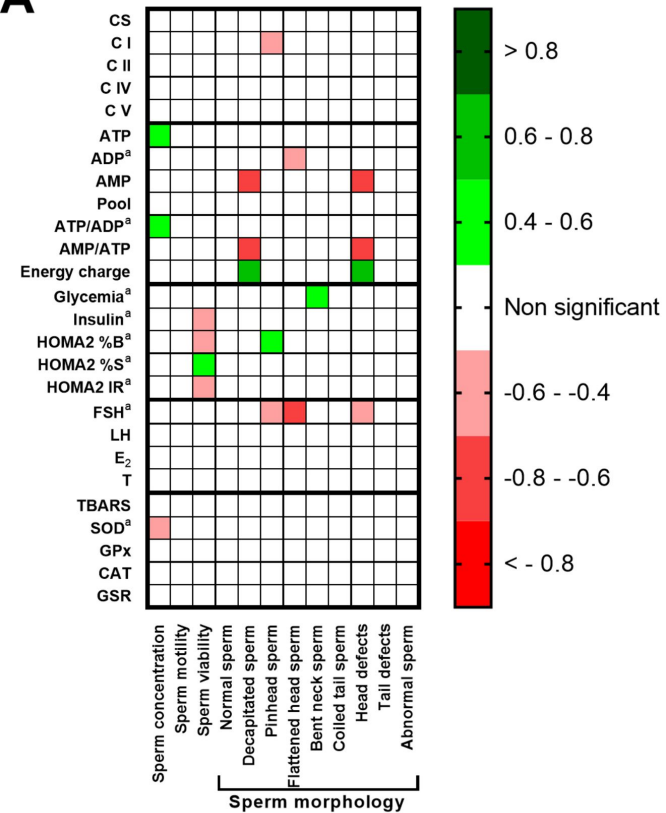
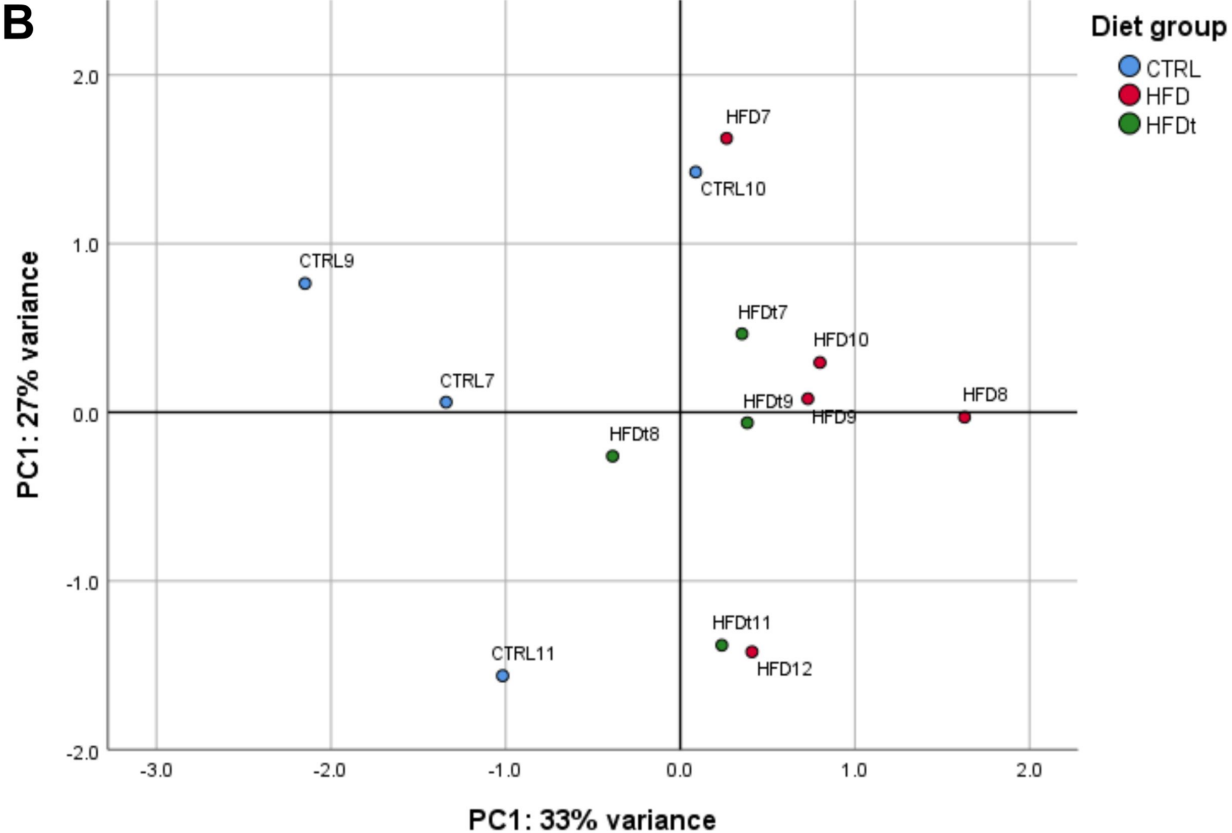
1124









A**B**

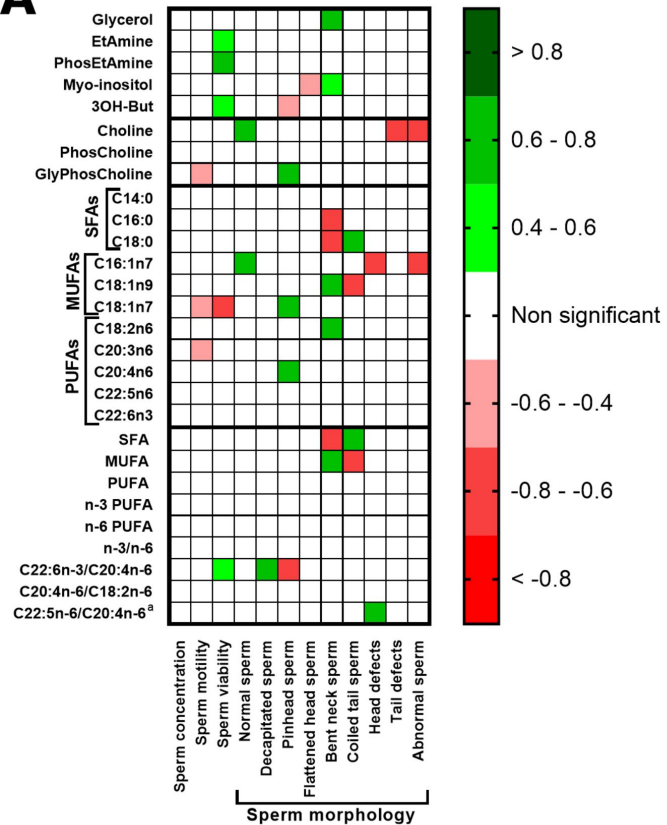
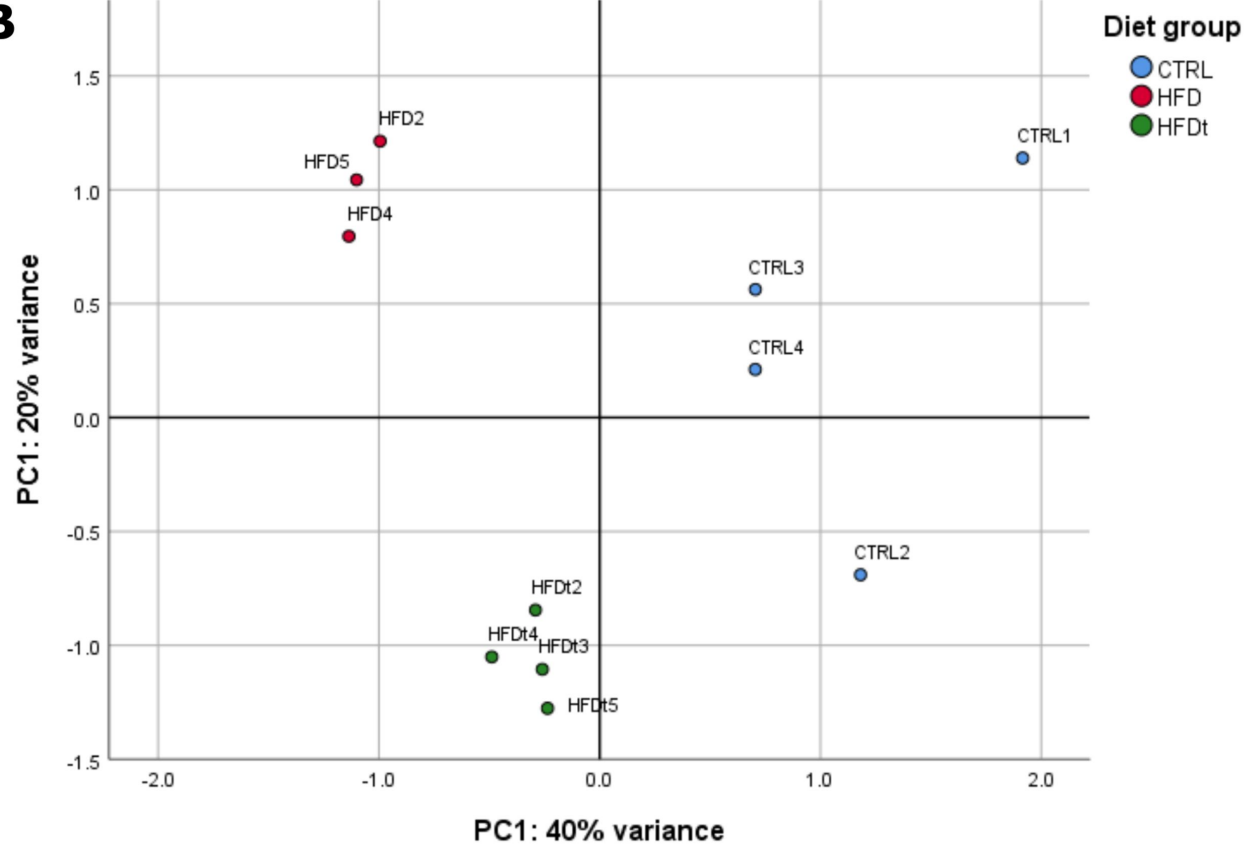
A**B**

Table 1: Fasting glycemia and serum concentrations of insulin, FSH, LH, 17 β -estradiol and testosterone in mice fed standard chow (CTRL), life-long high-fat diet (HFD), and those subjected to diet correction after 60 days (HFD_t). Fasting glycemia was evaluated using a glucometer (One Touch Ultra Lifescan-Johnson, Milpitas, CA, USA). Hormones were quantified by ELISA assay kits. Results are expressed as mean \pm standard deviation (units disclosed in the table). CTRL – standard chow; HFD – high-fat diet; HFD_t – transient high-fat diet. Data was tested by one-way ANOVA with Tukey’s HSD for group comparison. Significance was considered when $p < 0.05$. * vs. CTRL; # vs. HFD. * $p < 0.05$; ** $p < 0.01$; *** $p < 0.001$; **** $p < 0.0001$.

Analyte	CTRL (n=8)	HFD (n=8)	HFD _t (n=8)
<i>Fasting glucose (mg/dL)</i>	94.50 \pm 7.94	116.08 \pm 15.26 ***	84.91 \pm 9.91 ####
<i>Insulin (nmol/mL)</i>	0.49 \pm 0.68	3.56 \pm 1.75 ****	0.67 \pm 0.25 #####
<i>FSH (nmol/mL)</i>	6.60 \pm 2.83	4.25 \pm 3.18	3.77 \pm 2.67
<i>LH (nmol/mL)</i>	435.99 \pm 79.50	406.89 \pm 61.62	470.30 \pm 28.34
<i>17β-estradiol (pmol/mL)</i>	348.89 \pm 46.55	335.46 \pm 114.04	413.87 \pm 108.97
<i>Testosterone (nmol/mL)</i>	15.88 \pm 0.58	15.88 \pm 0.48	15.23 \pm 0.97

Table 2: Sperm morphology distribution, according to different classifications, in mice fed standard chow (CTRL), life-long high-fat diet (HFD), and those subjected to diet correction after 60 days (HFD_t). Results are expressed as mean (% of total sperm cells) ± standard deviation. CTRL – standard chow; HFD – high-fat diet; HFD_t – transient high-fat diet. Sperm count distributions across groups were tested using the χ^2 test. Differences between groups for each morphological classification were tested by one-way ANOVA with Tukey's HSD. For both methods, significance was considered when $p < 0.05$. * vs. CTRL; # vs. HFD. * $p < 0.05$; ** $p < 0.01$; *** $p < 0.001$; **** $p < 0.0001$.

Sperm Morphology	CTRL (n=9)	HFD (n=12)	HFD_t (n=9)	χ^2 test
<i>Normal (%)</i>	39.79 ± 6.01	33.82 ± 6.74	36.51 ± 4.08	
<i>Decapitated (%)</i>	12.10 ± 5.27	11.19 ± 3.61	12.18 ± 3.11	
<i>Pinhead (%)</i>	3.70 ± 1.30	6.20 ± 1.26**	6.68 ± 1.94**	106.83 ****
<i>Flattened head (%)</i>	3.92 ± 0.76	4.62 ± 1.20	6.02 ± 0.86***.#	
<i>Bent neck (%)</i>	6.49 ± 0.97	9.38 ± 3.64	5.30 ± 1.97##	
<i>Coiled tail (%)</i>	34.00 ± 5.73	34.77 ± 7.06	33.32 ± 2.46	
<i>Normal (%)</i>	39.79 ± 6.01	33.82 ± 6.74	36.51 ± 4.08	
<i>Head defects (%)</i>	19.72 ± 3.82	22.03 ± 4.52	24.88 ± 2.45*	48.57 ****
<i>Tail defects (%)</i>	40.49 ± 5.58	44.15 ± 6.41	38.61 ± 3.00	
<i>Normal (%)</i>	39.79 ± 6.01	33.82 ± 6.74	36.51 ± 4.08	26.16 ****
<i>Abnormal (%)</i>	60.21 ± 6.01	66.18 ± 6.74	63.49 ± 4.08	

Table 3: Polar lipid metabolites detected by $^1\text{H-NMR}$ in testicular extracts of mice fed standard chow (CTRL), life-long high-fat diet (HFD), and those subjected to diet correction after 60 days (HFD_t). Results are expressed as mean (arbitrary units) \pm standard deviation. CTRL – standard chow; HFD – high-fat diet; HFD_t – transient high-fat diet. Results were tested by one-way ANOVA with Tukey's HSD, except where stated otherwise. Significance was considered when $p < 0.05$. * vs. CTRL; # vs. HFD. * $p < 0.05$; ** $p < 0.01$; *** $p < 0.001$; **** $p < 0.0001$.

	Metabolite	CTRL (n=6)	HFD (n=6)	HFD _t (n=5)
Lipid intermediaries	<i>Glycerol</i>	$7.50 \times 10^{-3} \pm 8.48 \times 10^{-4}$	$9.26 \times 10^{-3} \pm 2.58 \times 10^{-4}$ **	$7.82 \times 10^{-3} \pm 7.14 \times 10^{-4}$ ##
	<i>Ethanolamine</i> ^a	$1.75 \times 10^{-3} \pm 2.21 \times 10^{-4}$	$1.74 \times 10^{-3} \pm 1.45 \times 10^{-4}$	$1.48 \times 10^{-3} \pm 1.31 \times 10^{-4}$ *, #
	<i>Phosphoethanolamine</i>	$2.01 \times 10^{-2} \pm 1.75 \times 10^{-3}$	$2.01 \times 10^{-2} \pm 5.93 \times 10^{-4}$	$1.99 \times 10^{-2} \pm 9.14 \times 10^{-4}$
	<i>Myo-inositol</i>	$4.94 \times 10^{-3} \pm 4.85 \times 10^{-4}$	$5.54 \times 10^{-3} \pm 2.69 \times 10^{-4}$ *	$4.58 \times 10^{-3} \pm 3.16 \times 10^{-4}$ ##
	<i>3-Hydroxybutyrate</i>	$6.68 \times 10^{-2} \pm 1.08 \times 10^{-2}$	$5.70 \times 10^{-2} \pm 3.40 \times 10^{-3}$	$5.97 \times 10^{-2} \pm 6.44 \times 10^{-3}$
Choline metabolism	<i>Choline</i>	$1.32 \times 10^{-2} \pm 1.56 \times 10^{-3}$	$0.98 \times 10^{-2} \pm 1.29 \times 10^{-3}$ **	$1.12 \times 10^{-2} \pm 1.32 \times 10^{-3}$
	<i>Phosphocholine</i>	$2.01 \times 10^{-2} \pm 1.75 \times 10^{-3}$	$2.01 \times 10^{-2} \pm 5.93 \times 10^{-4}$	$1.99 \times 10^{-2} \pm 9.14 \times 10^{-4}$
	<i>Glycerophosphocholine</i>	$3.00 \times 10^{-3} \pm 3.39 \times 10^{-4}$	$4.26 \times 10^{-3} \pm 3.70 \times 10^{-4}$ ****	$3.81 \times 10^{-3} \pm 2.67 \times 10^{-4}$ *

^a Kruskal-Wallis test, unadjusted p-value.